

On the Uncertainty of Large Language Model-Based Multi-Agent Systems

Yuxuan Zhao^{1,2} Sijia Chen² Ningxin Su²

Abstract

Multi-agent systems (MAS) have emerged as a prominent paradigm for leveraging large language models (LLMs) to tackle complex tasks. However, the mechanisms governing the effectiveness of MAS built upon publicly available LLMs, specifically the underlying rationales for their success or failure, remain largely unexplored. In this paper, we revisit MAS through the perspective of *uncertainty*, considering both intra- and inter-agent dynamics by investigating entropy transitions during problem-solving across various topologies and six benchmark tasks. By analyzing 245 features spanning token-, trajectory-, and round-level entropy, we counterintuitively find that a single agent outperforms MAS in approximately 43.3% of cases, and that uncertainty dynamics are largely determined during the first round of interaction. Furthermore, we provide three key observations: 1) *Certainty Preference*: reducing uncertainty at any stage for any agent is critical for guaranteeing correct solutions; 2) *Base Uncertainty*: base models with lower entropy during problem-solving directly benefit MAS performance; and 3) *Task Awareness*: entropy dynamics of MAS play varying roles across different tasks. Building on these insights, we introduce a simple yet effective algorithm, the *Entropy Judger*, to select solutions from MAS’s pass@ k results, leading to consistent accuracy improvements across all MAS configurations and tasks. Our source code is available at this [https URL](https://github.com/yuxuanzhao/MAS_Uncertainty).

1. Introduction

Multi-agent systems (MAS), with each agent built upon large language models (LLMs), are broadly applied in diverse domains (Du et al., 2023; Hong et al., 2023; Liu et al., 2023; Paglieri et al., 2024; Xu et al., 2024; Dang et al.,

¹Yantai Research Institute of Harbin Engineering University
²Hong Kong University of Science and Technology (Guangzhou). Correspondence to: Sijia Chen <sijiachen@hkust-gz.edu.cn>.

Preprint. February 5, 2026.

2025) and even regarded as the only choice for problem-solving (Zhang et al., 2024a). However, it remains largely unexplored whether MAS, particularly those built upon open-source LLMs, can outperform their single-agent counterparts, and what underlies their effectiveness.

Existing literature has observed that single-agent systems (SAS) can match or even surpass MAS on certain tasks (Gao et al., 2025; Li, 2026) and the failures of MAS often stem from communication breakdowns, inter-agent misalignment, and insufficient verification (Cemri et al., 2025). In particular, recent work establishes scaling principles for MAS through quantitative analysis (Kim et al., 2025). However, these studies are primarily conditioned on simple metrics such as accuracy, latency, and cost without providing a deeper understanding of the underlying mechanisms.

Meanwhile, alongside these advances, research into the reasoning of agentic LLMs has yielded further progress when uncertainty is incorporated into the analysis. By focusing exclusively on entropy, prior work has progressed from analyzing its role in reinforcement learning (RL) (Cui et al., 2025; Hao et al., 2025) to developing RL training algorithms that explicitly leverage entropy to balance exploration and exploitation (Chen et al., 2025a; Sharma & Chopra, 2025; Li et al., 2025; Zhang et al., 2025a; Zhu et al., 2025; Cao et al., 2025). Notably, even individual observations of correlations between entropy and accuracy have spawned distinct research directions, including entropy regularization (Zhang et al., 2025b; Chen et al., 2025b; Jiang et al., 2025), advantage shaping (Liu et al., 2025; Cheng et al., 2025), and entropy-guided token updates (Wang et al., 2025).

Therefore, for LLM-based MAS, which are inherently complex and exhibit uncertainty at the token, agent, and other levels, it is crucial to build a comprehensive relationship between uncertainty and reasoning reliability. Although the most recent work (He et al., 2025) provides analysis from an information-theoretic perspective, it remains limited to the compression-prediction pipeline and communication channels alone.

In this paper, we revisit MAS by investigating the entire life-cycle of uncertainty across diverse levels, steps, and phases involved in reasoning, under varying MAS topologies and tasks. Specifically, by mining the fine-grained correlation between large-scale information entropy, which is derived

from both intra-agent and inter-agent interactions, and MAS performance, we demonstrate that MAS effectiveness is largely determined by early-round uncertainty dynamics, with peak uncertainty universally harmful across architectures. In summary, our key contributions are:

- A systematic study of entropy dynamics across six benchmark tasks and four MAS topologies, analyzing 245 features at token, trajectory, and interaction-round levels;
- The counterintuitive finding that SAS outperform MAS in approximately 43.3% of cases, while reducing uncertainty to stable, low levels strongly correlates with correctness. This underscores the trade-off between system complexity and performance;
- Three insights on entropy behavior: Certainty Preference (reducing uncertainty at any stage strongly correlates with correctness), Base Uncertainty (lower initial entropy in agents enhances MAS gains), and Task Awareness (entropy patterns differ meaningfully across different tasks);
- The *Entropy Judger*, which selects high-quality outputs from MAS pass@ k results and consistently boosts accuracy across all configurations and tasks.

2. Related Work

Large Language Model-based Multi-Agent Systems (MAS) decompose complex tasks into specialized agents that interact through diverse coordination topologies (Chen et al., 2023; Zhang et al., 2024b; Dang et al., 2025; Zhang et al., 2025c), thereby enhancing problem-solving capabilities. Beyond improving accuracy and efficiency of MAS, several studies examine the conditions under which MAS are effective. Scaling analyses show that gains from adding agents or varying coordination structures are often offset by communication overhead and inter-agent misalignment, yielding diminishing or even negative returns (Kim et al., 2025). Recent work identifies key failure modes in MAS, such as insufficient verification and communication breakdowns (Cemri et al., 2025). More recently, SAS equipped with rich skill libraries have been shown to match or surpass MAS in both accuracy and efficiency (Li, 2026). While these works inform MAS practice, they rely on simple metrics that fail to capture system complexity and therefore cannot uncover the underlying rationales governing MAS effectiveness. Recent information-theoretic analysis (He et al., 2025) offers deeper insight but is limited to specific compressor-predictor architectures.

However, analyzing **uncertainty in LLM reasoning**, as quantified by policy entropy (Chen et al., 2025a; Cui et al., 2025; Cao et al., 2025; Zhu et al., 2025; Buffa & Del Corro, 2026), has deepened our understanding of the underlying reasoning process. In RL training, reducing entropy sharpens the output distribution and can improve accuracy (Karan & Du, 2025; Agarwal et al., 2025), but this benefit is highly

dependent on the base model capabilities, and aggressive entropy reduction may trigger *entropy collapse*, wherein the model becomes overconfident and converges to suboptimal policies (Yue et al., 2025; Zhang et al., 2025d; Chen et al., 2025b; Jiang et al., 2025). To mitigate this, recent work proposes entropy-intervention methods, including entropy regularization (Zhang et al., 2025b; Chen et al., 2025b; Jiang et al., 2025), entropy-based advantage shaping (Liu et al., 2025; Cheng et al., 2025), and entropy-guided token updates (Wang et al., 2025; Hao et al., 2025; Yang et al., 2025b). At test time, entropy also serves as an uncertainty signal to dynamically adjust reasoning depth and direction (Li et al., 2025; Sharma & Chopra, 2025; Liu et al., 2025). While these studies enhance single-agent reasoning by probing uncertainty, they largely overlook how uncertainty propagates across multiple interacting agents. Traditional multi-agent RL leverages uncertainty for exploration in continuous action spaces (Zhang et al., 2020; Sun et al., 2020; Kim & Sung, 2023), but such methods do not transfer to discrete, language-based coordination. To address this gap, we analyze uncertainty dynamics in LLM-based MAS to explain when and why these systems succeed.

3. Preliminaries

We consider a dataset $\mathcal{D} = \{(x_i, y_i^*)\}_{i=1}^N$, where x_i is a problem and y_i^* its verifiable ground-truth answer. Let M_{base} be an LLM with parameters θ , inducing a policy $\pi_\theta(v | s)$ over tokens $v \in \mathcal{V}$ given textual state s .

3.1. Single- and Multi-Agent Configurations

We define each system as $M = (A, G, \pi_\theta, \mathcal{M}, R)$, where A is a set of agents each built on M_{base} , $G = (A, E)$ is a directed interaction graph governing message passing, π_θ is the shared M_{base} policy, R is the number of interaction rounds, and $\mathcal{M} : A \times \{1, \dots, R\} \rightarrow 2^{\mathcal{T}}$ maps each agent-round pair to its context $\mathcal{H}_a^{(r)}$, a set of prior trajectories. Each agent generates a reasoning trajectory $\tau_a^{(r)} \sim \pi_\theta(\cdot | x, \mathcal{H}_a^{(r)})$, and the system outputs a final prediction \hat{y} .

Single Agent System (SAS). $A = \{a\}$, $G = (\{a\}, \emptyset)$. The agent accumulates its own history across rounds: $\mathcal{H}_a^{(r)} = \{\tau_a^{(r')}\}_{r' < r}$, with $\hat{y} = \tau_a^{(R)}$.

Sequential. $A = \{a_1, \dots, a_N\}$, G is a path $a_1 \rightarrow \dots \rightarrow a_N$. Within each round, agents pass messages along the path; across rounds, the first agent receives aggregated history:

$$\mathcal{H}_{a_j}^{(r)} = \begin{cases} \{\tau_a^{(r')}\}_{a \in A, r' < r} & j = 1, \\ \{\tau_{a_{j-1}}^{(r)}\} & j > 1, \end{cases} \text{with } \hat{y} = \tau_{a_N}^{(R)}.$$

Centralized. $A = A_{\text{work}} \cup \{a_o\}$ with working agents $A_{\text{work}} = \{w_1, \dots, w_N\}$ and orchestrator a_o . G is a star graph where all agents connect to a_o . The orchestrator aggregates agent outputs and broadcasts feedback: $\mathcal{H}_w^{(r)} = \{\tau_{a_o}^{(r-1)}\}$, $\mathcal{H}_{a_o}^{(r)} = \{\tau_w^{(r)}\}_{w \in A_{\text{work}}}$, with $\hat{y} = \tau_{a_o}^{(R)}$.

Debate. $A = \{a_1, \dots, a_N\}$, G is a directed path. Each agent observes all predecessors in the current round and all agents from previous rounds: $\mathcal{H}_{a_j}^{(r)} = \{\tau_{a_j'}^{(r')}\}_{j' < j} \cup \{\tau_a^{(r')}\}_{a \in A, r' < r}$. A non-LLM majority voting operator aggregates final answers: $\hat{y} = \mathcal{V}(\{\tau_a^{(R)}\}_{a \in A})$.

Hybrid. $A = A_{\text{work}} \cup \{a_o\}$ as in Centralized. Each working agent observes orchestrator feedback, all peer outputs from the previous round, and predecessors in the current round: $\mathcal{H}_{w_i}^{(r)} = \{\tau_{a_o}^{(r-1)}\} \cup \{\tau_w^{(r-1)}\}_{w \in A_{\text{work}}} \cup \{\tau_{w_j}^{(r)}\}_{j < i}$, $\mathcal{H}_{a_o}^{(r)} = \{\tau_w^{(r)}\}_{w \in A_{\text{work}}}$, with $\hat{y} = \tau_{a_o}^{(R)}$.

3.2. Uncertainty Metrics

Entropy has emerged as a fundamental perspective for understanding LLM reasoning (Li et al., 2025; Zhang et al., 2025a), with its dynamics directly influencing reasoning performance (Cui et al., 2025; Chen et al., 2025a). In contrast to these established roles in single-agent reasoning, we systematically analyze uncertainty in MAS through hierarchical entropy metrics, spanning token-, agent-, round-, sample-, and system-level granularities. Specifically, for any decoding state s , token-level entropy is $H(s) = -\sum_{v \in V} \pi_\theta(v | s) \log \pi_\theta(v | s)$. For sample i , agent $a \in A$, round r , and token position $k \in \tau_a^{(r)}$, we denote the decoding state as $s_k^{(i,a,r)}$ and its entropy as $H_k^{(i,a,r)} = H(s_k^{(i,a,r)})$. During experiments, we log $H_k^{(i,a,r)}$, time, and token costs for every agent at each round.

4. Exploring MAS with Uncertainty Dynamics

While prior work investigates failure modes of MAS (Cemri et al., 2025; Kim et al., 2025; Li, 2026), it relies on proprietary models and aggregate metrics, such as accuracy, latency, and cost, overlooking how uncertainty evolves within and across agents. We address this gap by analyzing entropy dynamics in open-source LLM-based MAS across diverse topologies and tasks.

4.1. Evaluation Protocol

Small, open-source LLMs enable cost-effective multi-agent collaboration through specialized task allocation and coordination (Shen et al., 2024; Chen & Varoquaux, 2024; Liang et al., 2024; Belcak et al., 2025). Their open access to token-level probabilities supports reliable uncertainty quantification, which is critical for agent decision-making. More discussion can be found in Appendix A.

To this end, in contrast to prior work (Kim et al., 2025) which evaluates only proprietary API-based models, our study focuses on publicly available LLMs, including the LLaMA series (3.1-8B-Instruct, 3.2-3B-Instruct) (Grattafiori et al., 2024) and the Qwen3 series (0.6B, 4B, 8B) (Yang et al., 2025a). All systems are built using the same M_{base} , with the number of interaction rounds fixed to 2, temperature set to 0.6, top- p to 0.95, and maximum sequence length to 8,192 tokens. Our evaluation

spans three domains: mathematics (GSM8K (Cobbe et al., 2021), MATH500 (Hendrycks et al., 2021b), AIME2024, AIME2025), code generation (HumanEval) (Chen, 2021), and knowledge QA (MMLU) (Hendrycks et al., 2021a). We use the first 100 samples for GSM8K and the first 1K samples for MMLU, while the full test sets are used for all other benchmarks. Each question is accompanied by a chain-of-thought prompt. On the challenging AIME24/25 benchmarks, the maximum sequence length is set to 16,384 tokens. We exclude debate architecture on HumanEval, as majority voting is generally ineffective for code generation tasks. Additional experimental details are provided in Appendix B.

4.2. Measuring Reasoning with Entropy and Beyond

Entropy has proven effective for analyzing single-agent reasoning (Sharma & Chopra, 2025; Zhu et al., 2025; Zhang et al., 2025a; Su et al., 2025). Recent work has even leveraged entropy-based features to train simple machine learning models that predict LLM correctness (Buffa & Del Corro, 2026). However, this approach is limited to a single LLM and computes entropy only from the top-20 token probabilities, yielding just 11 entropy-related features. We extend entropy analysis to MAS by designing hierarchical entropy features that capture how uncertainty evolves across agents and rounds. Specifically, for each sample i , agent $a \in A$, and round $r \in \{1, \dots, R\}$, we extract 254 features from logged traces:

Entropy features (\mathcal{F}_E , 239 features) measure uncertainty across hierarchical levels:

- *Agent-level statistics* capture per-agent reasoning trajectories, including their statistical properties, variations across rounds, and inter-agent entropy divergence (156);
- *Round-level dynamics* track aggregate entropy metrics for each round and their relative changes (27);
- *Sample-level statistics* aggregate entropy measures across all agents involved in processing a given sample (29);
- *System-level aggregation* provides global uncertainty measures by comparing entropy patterns across different coordination topologies (10);
- *Base-model entropy* ($\mathcal{F}_{\text{base-E}}$, 17 features) additionally captures uncertainty characteristics of M_{base} and quantifies shifts in entropy between M_{base} and MAS;

Computational metrics (\mathcal{F}_C , 15 features) capture non-entropy-related quantities, including reasoning time, token usage, inference counts, and M_{base} correctness ($\mathcal{F}_{\text{base-C}}$, 4 features), at the same hierarchical levels used for \mathcal{F}_E .

Excluding 9 experimental identifier columns yields 245 trainable features. We define three feature groups to isolate the influence of M_{base} on MAS performance: (1) **MAS only** (\mathcal{G}_{MAS} , $d = 224$): $\mathcal{G}_{\text{MAS}} = (\mathcal{F}_E \cup \mathcal{F}_C) \setminus (\mathcal{F}_{\text{base-E}} \cup \mathcal{F}_{\text{base-C}})$, capturing uncertainty dynamics intrinsic to multi-agent interaction; (2) **Base entropy** ($\mathcal{G}_{\text{base-H}}$, $d = 241$): $\mathcal{G}_{\text{base-H}} = \mathcal{G}_{\text{MAS}} \cup \mathcal{F}_{\text{base-E}}$, evaluating the impact of M_{base} entropy on MAS performance; (3) **Base full** ($\mathcal{G}_{\text{base-full}}$, $d = 245$):

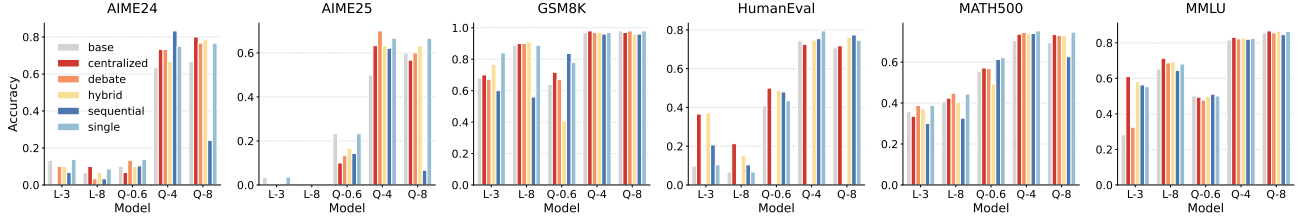


Figure 1. Accuracy comparison of SAS and MAS across models and datasets. For brevity, LLaMA-3.2-3B-Instruct and LLaMA-3.1-8B-Instruct are denoted as L-3 and L-8, respectively; Qwen3-0.6B, Qwen3-4B, and Qwen3-8B are denoted as Q-0.6, Q-4, and Q-8. The base denotes the accuracy of a single M_{base} on each dataset.

$\mathcal{G}_{\text{base-full}} = \mathcal{G}_{\text{base-H}} \cup \mathcal{F}_{\text{base-C}}$, directly measuring how M_{base} 's reasoning capability conditions or limits MAS effectiveness. Complete feature definitions are provided in Appendix C.

4.3. Mining Effectiveness of MAS

MAS built on LLMs inherently exhibit uncertainty during individual reasoning, and their interactions among agents compound this effect (Guo et al., 2024; Cemri et al., 2025; Gao et al., 2025; Tran et al., 2025). Prior work largely relies on simple metrics that fail to capture internal uncertainty dynamics or identify the factors underlying MAS failure. To address this, we leverage the hierarchical entropy features defined in Section 4.2 to reformulate MAS evaluation as a supervised learning problem: predicting per-sample correctness $y_i \in \{0, 1\}$ from entropy traces $\mathbf{x}_i \in \mathbb{R}^d$. This formulation enables data-driven mining through tree-based models, XGBoost (Chen, 2016) and LightGBM (Ke et al., 2017), to uncover fine-grained factors governing MAS effectiveness. Training on three feature groups with dimensions $d \in \{224, 241, 245\}$, we naturally derive the *Entropy Judger*, denoted as a classifier $f : \mathbb{R}^d \rightarrow [0, 1]$. Beyond binary prediction, f enables pass@ k selection on unseen configurations by identifying the candidate with the highest predicted probability of correctness: $\hat{\ell} = \arg \max_{\ell \in [k]} f(\mathbf{x}_\ell)$. To interpret learned patterns, we perform SHapley Additive exPlanations (SHAP) analysis (Lundberg & Lee, 2017) on both XGBoost and LightGBM. For each feature j , we extract two metrics: (1) **mean feature importance** $\bar{I}_j = \frac{1}{2} \sum_{m \in \mathcal{M}} \tilde{I}_j^{(m)}$, where $\tilde{I}_j^{(m)} \in [0, 1]$ is the min-max normalized importance from model $m \in \mathcal{M} = \{\text{XGBoost, LightGBM}\}$; and (2) **SHAP correlation** $\rho_j = \frac{1}{2} \sum_{m \in \mathcal{M}} \text{corr}(\mathbf{x}_j, \phi_j^{(m)})$, where \mathbf{x}_j denotes feature values and $\phi_j^{(m)}$ their SHAP attributions under model m . The sign of ρ_j indicates direction: $\rho_j > 0$ implies higher feature values increase predicted correctness. Further details are provided in Appendix B.4.

4.4. Examining Uncertainty Impacts on MAS

MAS does not always outperform SAS. Conventional assumptions suggest that more agents improve MAS performance (Zhang et al., 2024a). However, consistent with recent findings (Kim et al., 2025), we show that MAS does not

universally surpass SAS, and we substantially extend this observation to open-source LLMs across a broader range of tasks. Specifically, across 5 models and 6 datasets, SAS achieves the highest accuracy in 13 cases (43.3%) and outperforms at least one MAS architecture in 13 additional cases, totaling 26 out of 30 scenarios where SAS matches or exceeds MAS, shown in Figure 1. In the 13 cases where SAS is best, it surpasses the average MAS accuracy by 6.28%, primarily on math tasks and smaller models.

Base model entropy limits MAS effectiveness. Prior work shows MAS performance depends on M_{base} capability (Zhang et al., 2025c), a trend we also observe in Figure 1; moreover, we find that M_{base} uncertainty further constrains MAS effectiveness. On $\mathcal{G}_{\text{base-H}}$, the top predictors are total token-level entropy and answer length: for LLaMA, total token count ($\rho \approx -0.47$, $\bar{I} = 1.0$) and entropy ($\rho \approx -0.73$, $\bar{I} \approx 0.72$); for Qwen3, answer token count ($\rho \approx -0.18$, $\bar{I} \approx 0.58$) and entropy ($\rho \approx -0.64$, $\bar{I} \approx 0.36$). Critically, higher M_{base} entropy consistently reduces MAS accuracy across both families, as shown in Figure 2(b,d), with performance dropping sharply when entropy exceeds 100. Notably, despite this shared trend, entropy scales differ: LLaMA operates in low-entropy ranges (0-100) but achieves lower accuracy, while Qwen uses higher entropy (100-1,000) yet performs better. This reflects divergent reasoning styles, as Qwen tends to verify and refine its answers before producing a final output, generating self-correcting trajectories that yield more reliable results and suppress error propagation in MAS, even though this process incurs higher entropy, whereas LLaMA tends to accept and reuse answers from other agents without verification, leading to uncontrolled error propagation. We provide additional results in Appendix D.1 and an illustrative example in Appendix E.

MAS mainly fails on inter-agent misalignment. Prior work identifies inter-agent misalignment as a key cause of MAS failure (Cemri et al., 2025). We deepen this understanding by analyzing fine-grained entropy dynamics within MAS. On \mathcal{G}_{MAS} , as shown in Figure 3, we examine the top entropy-related features ranked by \bar{I} . For Qwen, failure is driven by high entropy variance across agents during

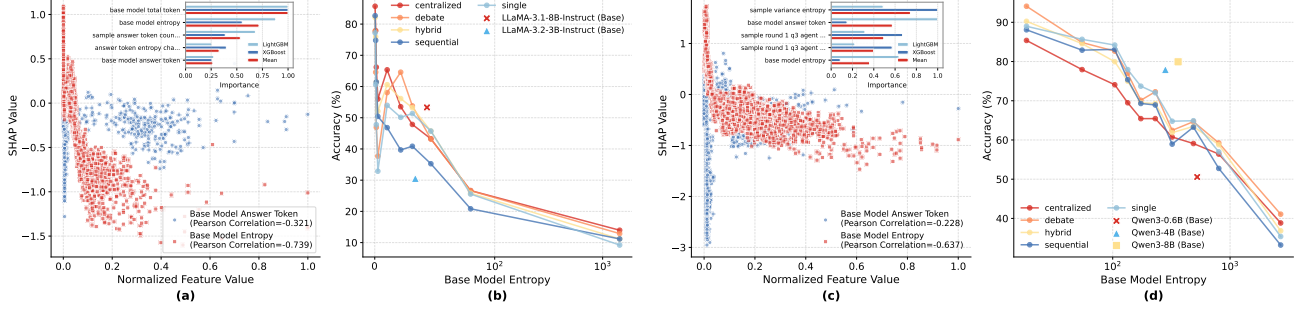


Figure 2. Base model entropy limits MAS effectiveness. The left two subfigures show results for LLaMA; the right two for Qwen. (a) Relationship between feature values and SHAP values for most important entropy features on $\mathcal{G}_{\text{base-H}}$, sorted by \bar{I}_j and annotated with ρ_j . (b) MAS performance across deciles of M_{base} entropy: M_{base} entropy is partitioned into ten equal-sized bins, and average MAS accuracy (aggregated over datasets and model sizes) is computed per bin. Additionally, the average M_{base} entropy and accuracy across all datasets are overlaid as markers.

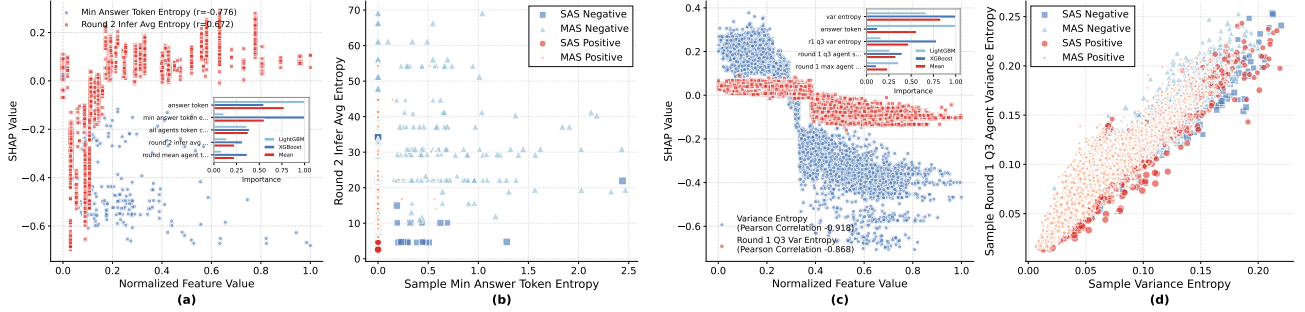


Figure 3. MAS mainly fails on inter-agent misalignment. The left two subfigures show results for LLaMA; the right two for Qwen. (a) Same as Figure 2(a), but for entropy features in \mathcal{G}_{MAS} . (b) Impact of these features on sample predicted correctness: for each sample in the LightGBM and XGBoost test sets, we plot feature values against the average predicted probability of correctness from both models.

problem solving ($\rho \approx -0.92$, $\bar{I} \approx 0.83$) and strong agent disagreement in round 1 (measured by third-quartile entropy variance: $\rho \approx -0.87$, $\bar{I} \approx 0.47$), indicating that early divergence leads to increasingly incompatible reasoning trajectories. This pattern is further corroborated in Figure 3 (d): at comparable levels of entropy variance, SAS exhibits consistently lower agent disagreement in round 1 than MAS, partially explaining SAS’s superior performance. In contrast, LLaMA failures are characterized by verbose and uncertain final answers, with answer-token count ($\rho \approx -0.63$, $\bar{I} \approx 0.78$) and minimum answer-token entropy ($\rho \approx -0.78$, $\bar{I} \approx 0.56$) as dominant predictors. Notably, for LLaMA, average per-agent entropy in round 2 shows a positive correlation with correctness, a pattern absent in Qwen, suggesting that higher uncertainty in later rounds reflects productive exploration rather than confusion, whereas Qwen achieves reliability through early convergence. More analysis can be found in the Appendix D.2.

5. Deep Analysis

5.1. Effective MAS Requires Stable Deliberation

Based on average MAS accuracy across datasets, we categorize mathematical reasoning tasks into three difficulty

levels: easy (GSM8K), medium (Math500), and hard (AIME24/25). We analyze entropy features in \mathcal{G}_{MAS} across these levels to understand how uncertainty shapes MAS effectiveness under varying task difficulty.

Stable and Low Entropy for Simple Problems. On GSM8K, the top features include final answer length and dispersion of early-round agent uncertainty (with $\bar{I} \in [0.51, 0.56]$ and $|\rho| \leq 0.15$), indicating only a mild influence on predicted correctness. In contrast, overall round-1 entropy ($\bar{I} \approx 0.47$, $\rho \approx -0.64$) and the stability index which measures consistency of entropy across agents ($\bar{I} \approx 0.44$, $\rho \approx -0.79$), are both highly predictive and strongly negatively correlated with success. This suggests that simple problems are best solved when agents converge quickly to low-entropy, stable answers.

Balanced Exploration for Medium Problems. On Math500, high average per-agent reasoning entropy ($\bar{I} \approx 0.77$, $\rho \approx 0.63$) and longer reasoning time in round 1 ($\bar{I} \approx 0.15$, $\rho \approx 0.71$) correlate positively with MAS success, suggesting that medium-difficulty problems benefit from sustained, moderately uncertain exploration. Conversely, excessive early uncertainty, measured by maximum

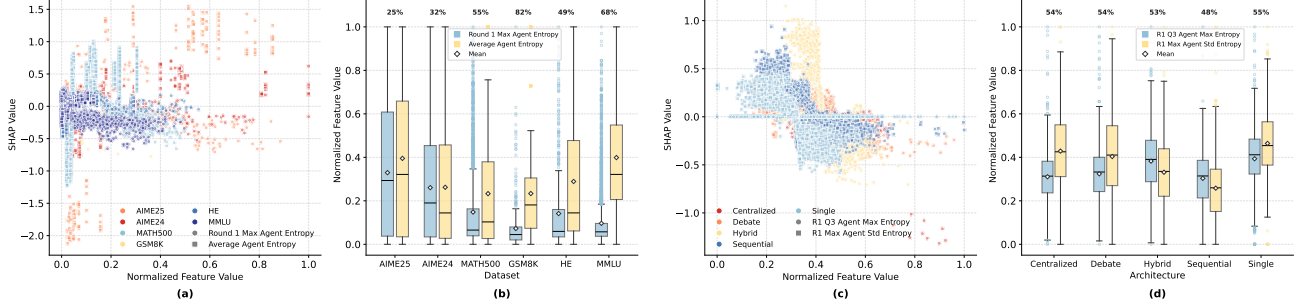


Figure 4. Uncertainty in MAS exerts distinct effects depending on task difficulty and the coordination architecture. (a, c) Feature-SHAP relationships for top entropy features in \mathcal{G}_{MAS} , grouped by dataset (a) and architecture (c). (b, d) Corresponding box plots across all models, annotated with average MAS correctness per dataset (b) or per architecture (d).

total entropy across agents in round 1 ($\rho \approx -0.73$), and verbose final answers ($\rho \approx -0.48$) strongly predict failure. Notably, median round-1 entropy also shows a negative correlation ($\rho \approx -0.36$), indicating that while some uncertainty aids discovery, uncontrolled divergence hinders consensus. Together, these findings show that on medium-difficulty problems, MAS succeeds when agents explore long enough with moderate uncertainty, but avoid excessive early divergence, and converge on a concise answer.

Structured Deliberation for Hard Problems. On AIME24/25, round-1 total reasoning time is the top predictor ($\bar{I} = 1.0$, $\rho \approx 0.73$), confirming that olympiad-level problems require substantial early effort. Crucially, entropy-related features reveal a sharp trade-off: excessive early uncertainty harms performance, evident in strong negative correlations for round-1 max entropy ($\rho \leq -0.70$) and per-token entropy ($\rho \approx -0.37$), while moderate average output entropy shows a positive correlation ($\rho \geq 0.37$). Entropy dispersion in later rounds also degrades accuracy, with high inter-agent variance in round-2 strongly predicting failure ($|\rho| \geq 0.66$). Together, these results show that success on hard problems demands not just long reasoning, but controlled uncertainty: early exploration must be bounded, and agent uncertainty must remain aligned.

Stable Uncertainty for Code Generation. On HumanEval, total reasoning time is the strongest predictor, and moderate average entropy improves performance, while both overconfident and erratic uncertainty profiles degrade it. This echoes the principle observed in mathematical reasoning: deliberation benefits MAS only when uncertainty remains structured and stable.

Inter-Agent Agreement for Knowledge QA. On MMLU, MAS performance depends on inter-agent agreement, not deliberation length. Entropy variance is the top predictor, and larger teams reduce accuracy. Unlike in math or code, slightly longer answers help, though high-entropy tails remain harmful. Extended interaction yields no benefit, confirming that consensus, not duration, drives success in

knowledge-intensive QA.

Overall, **entropy-performance relationships are task-aware**: simple tasks demand rapid convergence to low, stable entropy, whereas medium and hard tasks benefit from moderate average entropy but are harmed by peak or dispersed uncertainty. This reveals that harder problems require more exploratory reasoning, yet uncontrolled entropy spikes remain universally detrimental. Additionally, **extended reasoning consistently improves MAS performance on hard tasks**, with trajectory length strongly predictive of success ($\bar{I} \geq 0.75$, $\rho \geq 0.63$). This aligns with findings in LLM reinforcement learning, where longer reasoning chains reflect stronger underlying reasoning capabilities (Yeo et al., 2025; Chen et al., 2025c). Beyond per-dataset analyses, we examine the two most important entropy features across all models and datasets: round-1 maximum agent entropy and average entropy of agents’ outputs during problem solving. Figure 4(a) shows that harder tasks exhibit wider SHAP value distributions and benefit from moderate average entropy, whereas high early uncertainty consistently harms performance. In contrast, easier datasets gain little from higher entropy. Figure 4(b) further reveals that as dataset accuracy declines, from 82% on GSM8K to 25% on AIME25, both entropy features increase in magnitude and dispersion, with round-1 max entropy showing the strongest sensitivity to task difficulty. This suggests that difficult problems not only induce higher uncertainty, but also amplify inter-agent disagreement, making early entropy control increasingly critical as task complexity grows. Finally, these results show that **MAS succeeds by reasoning more while keeping uncertainty low and consistent across agents**. We show these findings with token-level entropy case studies in Appendix F and provide further analysis in Appendix D.3.

5.2. Peak Entropy Is Universally Harmful in MAS

We analyze how entropy features influence MAS effectiveness across five architectures on \mathcal{G}_{MAS} .

Centralized systems are highly sensitive to early uncertainty: peak agent entropy in round 1 and peak answer entropy strongly predict failure, as the orchestrator’s single-

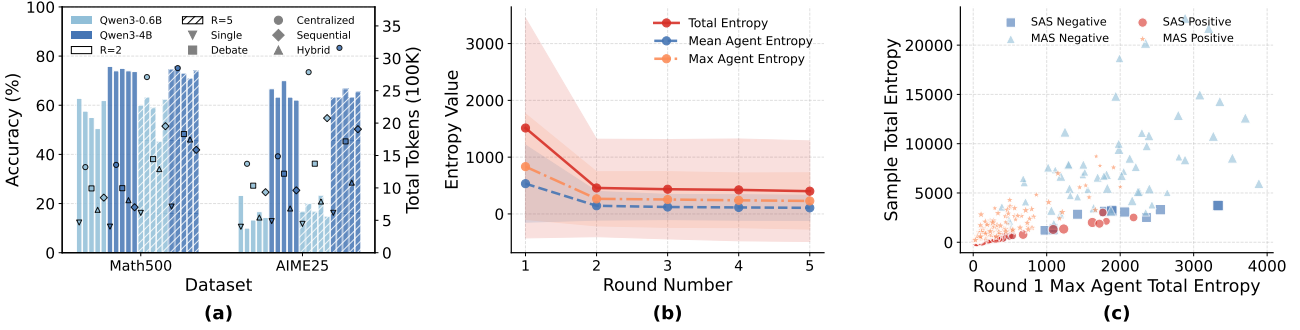


Figure 5. More rounds do not necessarily improve MAS performance. (a) Accuracy and token consumption for different MAS architectures with $R = 2$ and $R = 5$ on two benchmarks. (b) Evolution of three key entropy metrics across rounds. (c) The impact of two prominent entropy features, notable for their high importance (\bar{I}) and strong correlation ($|\rho|$) with sample correctness.

context aggregation allows any erratic agent to contaminate the entire reasoning process. **Debate** architectures depend critically on early consensus: high initial agent divergence reflect how initial divergence amplifies across rounds, preventing convergence; yet once aligned, cumulative entropy becomes beneficial, indicating productive exploration. **Hybrid** systems balance robustness and depth: early peak entropy remains harmful, but dual feedback from peers and orchestrator enables recovery through extended deliberation. **Sequential** systems are most fragile: answer-level entropy dominates the top predictors, reflecting error propagation through strict role chaining with no cross-checking. **Single (SAS)** prioritize brevity and penalize both high answer entropy and entropy variance, indicating that internal consistency is critical for success.

Architecture determines which entropy matters. Aggregation-based systems (centralized, debate) fail on inter-agent dispersion, as noisy inputs corrupt shared contexts. Sequential systems fail on answer-level entropy, where specialized roles propagate errors without cross-verification. Hybrid systems are most robust, reconciling conflicts through dual feedback. **Universally, peak entropy harms, while cumulative entropy helps**, showing MAS succeeds by shaping entropy distribution, not eliminating uncertainty. Beyond per-architecture analysis, we compare two key features across all architectures: upper-quartile agent peak entropy and maximum entropy dispersion across agents in round 1. Figure 4(c) shows both negatively predict correctness within each architecture. Surprisingly, Figure 4(d) reveals an inverse trend across architectures: sequential (lowest-performing) shows lowest feature averages, while single (highest-performing) shows highest. This indicates that **the relationship between entropy and performance depends on architectural capacity to control uncertainty**, not merely on minimizing entropy. More analysis can be found in Appendix D.4.

5.3. More Rounds Are Not Always Better

All experiments above default to $R = 2$ rounds. To investigate whether more rounds help, we extend analysis to $R = 5$ using Qwen3-0.6B and Qwen3-4B on MATH500 (first 100 samples) and AIME2025, expanding the feature space from 224 to 494 dimensions.

Comparing $R = 2$ and $R = 5$, we find that **extending deliberation rarely improves performance and often harms it**, even at the cost of higher token consumption, as shown in Figure 5(a). On challenging benchmarks like AIME25 and MATH500, most architectures, including debate and hybrid, exhibit performance degradation with additional rounds, especially for smaller models. The only consistent gains occur in centralized systems, where strong orchestration enables effective aggregation over longer trajectories. In contrast, peer-based architectures (debate, hybrid) appear to suffer from prolonged disagreement, as repeated interactions without convergence amplify noise rather than refine reasoning. This is further supported by entropy dynamics: as Figure 5(b) shows, key uncertainty metrics, maximum, mean, and total entropy, drop sharply from round 1 to round 2, but remain nearly flat from round 2 to round 5, indicating that agents largely stabilize after the second round. Together, these results demonstrate that simply increasing the number of rounds does not enhance MAS performance; instead, **the benefit of extended deliberation depends critically on an architecture's ability to align agents and stabilize uncertainty early in the process**.

Despite the expanded feature space with $R = 5$, early-round uncertainty remains the dominant failure mode, as shown in Figure 5(c). Round-1 features dominate the top predictors: peak cumulative agent entropy in round 1 ranks second ($\bar{I} \approx 0.60$, $\rho \approx -0.91$), and upper-quartile inter-agent entropy dispersion also appears in the top five ($\bar{I} \approx 0.50$), underscoring the critical role of early consensus. Even cumulative sample-level entropy is strongly harmful ($\rho \approx -0.73$), reinforcing that uncontrolled uncertainty, not just its timing, is detrimental. These results confirm a central

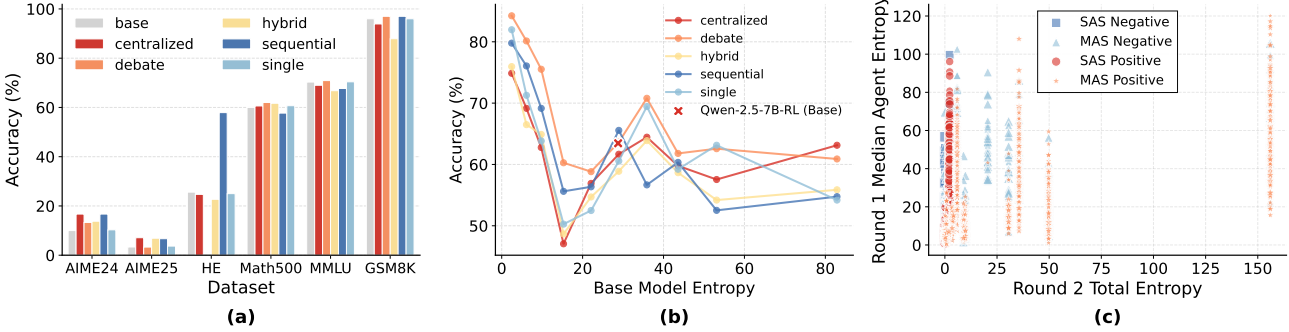


Figure 6. The role of uncertainty is reshaped in MAS built on Qwen2.5-7B-SimpleRL-Zoo. (a) The performance of different MAS architectures across datasets. (b) Relationship between base-model entropy and MAS accuracy. (c) Most predictive features in \mathcal{G}_{MAS} .

principle: **MAS effectiveness is largely determined in the first round, and additional deliberation cannot reliably recover from initial misalignment.** More analysis can be found in Appendix D.5.

5.4. RL Training Inverts the Role of Uncertainty

Few studies have investigated whether using a specialized, fine-tuned model as the base can improve MAS performance on reasoning tasks. We explore this using Qwen2.5-7B-SimpleRL-Zoo (Zeng et al., 2025), denoted $M_{\text{RL-base}}$, an RL-fine-tuned model trained on 8K MATH problems.

Figure 6 highlights three findings. (1) $M_{\text{RL-base}}$ consistently enables MAS to outperform SAS, whereas with the standard M_{base} , SAS surpasses MAS in 43.3% of cases, but never does with $M_{\text{RL-base}}$. (2) **The base model entropy-accuracy relationship is reshaped:** for M_{base} , higher entropy monotonically reduces accuracy, but for $M_{\text{RL-base}}$, accuracy first declines then recovers with increasing entropy, as shown in Figure 6(b), indicating that moderate uncertainty supports productive exploration. (3) On \mathcal{G}_{MAS} , the top predictors are round-1 median entropy ($\rho \approx -0.758$) and round-2 entropy ($\rho \approx 0.267$), as shown in Figure 6(c), suggesting early convergence is beneficial, while later entropy reflects refinement rather than noise.

Further comparison across Figure 2(b,d) and Figure 6(b) shows that $M_{\text{RL-base}}$ achieves both lower entropy and higher correctness than M_{base} . This indicates that RL training yields better reasoning and more reliable uncertainty estimates. Unlike standard models, where high entropy often signals hallucination, $M_{\text{RL-base}}$ harnesses uncertainty to drive effective exploration, enabling MAS to generate diverse, valuable reasoning paths that are iteratively refined. Consequently, MAS leverages this enhanced base capability to outperform SAS. More analysis can be found in Appendix D.6.

5.5. Uncertainty Predicts MAS Correctness

The *Entropy Judger* achieves strong classification accuracy using only MAS-derived entropy features from \mathcal{G}_{MAS} , as shown in Table 1, demonstrating that uncertainty dynamics

Table 1. *Entropy Judger* cross-validation accuracy. Results are averaged over five folds, and standard deviations are below 0.02 across all settings; these values are omitted for brevity.

Feature Group	Description	LLaMA	Qwen
\mathcal{G}_{MAS}	MAS only	0.726	0.791
$\mathcal{G}_{\text{base-H}}$	+ base entropy	0.745	0.807
$\mathcal{G}_{\text{base-full}}$	+ base correctness	0.812	0.916

alone are highly predictive of correctness. Beyond binary prediction, the *Entropy Judger* enables label-free pass@ k selection and consistently improves accuracy across all MAS configurations. Incorporating base model features from $\mathcal{G}_{\text{base-H}}$ and $\mathcal{G}_{\text{base-full}}$ yields further gains, confirming that base model characteristics influence MAS effectiveness. This practical capability, selecting high-quality outputs without ground-truth labels, makes the *Entropy Judger* well suited for real-world deployment. Additional details are provided in Appendix G.

6. Conclusion

This study presents a comprehensive analysis of uncertainty dynamics in LLM-based multi-agent systems, examining 245 entropy features across six benchmarks and four MAS topologies. Our findings challenge prevailing assumptions: single agents outperform MAS in 43.3% of cases, and MAS effectiveness is largely determined by first-round entropy dynamics rather than extended deliberation. We identify three principles governing MAS performance: (1) *Certainty Preference*, where reducing uncertainty at any stage correlates with correctness; (2) *Base Uncertainty*, where lower base model entropy directly benefits MAS; and (3) *Task Awareness*, where optimal entropy profiles vary by task difficulty. Building on these insights, the *Entropy Judger* leverages learned entropy patterns to select high-quality outputs from MAS pass@ k candidates, achieving consistent accuracy gains without ground-truth labels. Our work establishes uncertainty as a principled perspective for understanding and improving multi-agent reasoning.

Impact Statement

This work provides a principled understanding of uncertainty dynamics in LLM-based multi-agent systems, offering practical value for both researchers and practitioners. For the research community, our entropy-based analysis framework establishes a new perspective for diagnosing MAS failures and guiding architectural design decisions. For practitioners, our findings that single agents outperform MAS in 43.3% of cases, combined with the insight that first-round dynamics largely determine outcomes, can inform more resource-efficient deployment strategies. The *Entropy Judger* further enables quality-aware output selection without requiring ground-truth labels, reducing annotation costs in real-world applications. We do not foresee specific negative societal consequences beyond those generally associated with advancing LLM capabilities.

References

- Agarwal, S., Zhang, Z., Yuan, L., Han, J., and Peng, H. The unreasonable effectiveness of entropy minimization in llm reasoning. *arXiv preprint arXiv:2505.15134*, 2025.
- Belcak, P., Heinrich, G., Diao, S., Fu, Y., Dong, X., Muralidharan, S., Lin, Y. C., and Molchanov, P. Small language models are the future of agentic ai. *arXiv preprint arXiv:2506.02153*, 2025.
- Buffa, P. M. and Del Corro, L. Entropy sentinel: Continuous llm accuracy monitoring from decoding entropy traces in stem. *arXiv preprint arXiv:2601.09001*, 2026.
- Cao, H., Bai, Z., Peng, Z., Wang, B., Yang, T., Huo, J., Zhang, Y., and Gao, Y. Efficient reinforcement learning with semantic and token entropy for llm reasoning. *arXiv preprint arXiv:2512.04359*, 2025.
- Cemri, M., Pan, M. Z., Yang, S., Agrawal, L. A., Chopra, B., Tiwari, R., Keutzer, K., Parameswaran, A., Klein, D., Ramchandran, K., et al. Why do multi-agent llm systems fail? *arXiv preprint arXiv:2503.13657*, 2025.
- Chen, L. and Varoquaux, G. What is the role of small models in the llm era: A survey. *arXiv preprint arXiv:2409.06857*, 2024.
- Chen, M. Evaluating large language models trained on code. *arXiv preprint arXiv:2107.03374*, 2021.
- Chen, M., Chen, G., Wang, W., and Yang, Y. Seed-grpo: Semantic entropy enhanced grpo for uncertainty-aware policy optimization. *arXiv preprint arXiv:2505.12346*, 2025a.
- Chen, P., Li, X., Li, Z., Yin, W., Chen, X., and Lin, T. Exploration vs exploitation: Rethinking rlr through clipping, entropy, and spurious reward. In *The 5th Workshop on Mathematical Reasoning and AI at NeurIPS 2025*, 2025b.
- Chen, Q., Qin, L., Liu, J., Peng, D., Guan, J., Wang, P., Hu, M., Zhou, Y., Gao, T., and Che, W. Towards reasoning era: A survey of long chain-of-thought for reasoning large language models. *arXiv preprint arXiv:2503.09567*, 2025c.
- Chen, T. Xgboost: A scalable tree boosting system. *Cornell University*, 2016.
- Chen, W., Su, Y., Zuo, J., Yang, C., Yuan, C., Chan, C.-M., Yu, H., Lu, Y., Hung, Y.-H., Qian, C., et al. Agentverse: Facilitating multi-agent collaboration and exploring emergent behaviors. In *The Twelfth International Conference on Learning Representations*, 2023.
- Cheng, D., Huang, S., Zhu, X., Dai, B., Zhao, W. X., Zhang, Z., and Wei, F. Reasoning with exploration: An entropy perspective. In *Annual AAAI Conference on Artificial Intelligence*, 2025.
- Cobbe, K., Kosaraju, V., Bavarian, M., Chen, M., Jun, H., Kaiser, L., Plappert, M., Tworek, J., Hilton, J., Nakano, R., et al. Training verifiers to solve math word problems. *arXiv preprint arXiv:2110.14168*, 2021.
- Cui, G., Zhang, Y., Chen, J., Yuan, L., Wang, Z., Zuo, Y., Li, H., Fan, Y., Chen, H., Chen, W., et al. The entropy mechanism of reinforcement learning for reasoning language models. *arXiv preprint arXiv:2505.22617*, 2025.
- Dang, Y., Qian, C., Luo, X., Fan, J., Xie, Z., Shi, R., Chen, W., Yang, C., Che, X., Tian, Y., et al. Multi-agent collaboration via evolving orchestration. In *Advances in neural information processing systems*, 2025.
- Du, Y., Li, S., Torralba, A., Tenenbaum, J. B., and Mordatch, I. Improving factuality and reasoning in language models through multiagent debate. In *Forty-first International Conference on Machine Learning*, 2023.
- Gao, M., Li, Y., Liu, B., Yu, Y., Wang, P., Lin, C.-Y., and Lai, F. Single-agent or multi-agent systems? why not both? *arXiv preprint arXiv:2505.18286*, 2025.
- Grattafiori, A., Dubey, A., Jauhri, A., Pandey, A., Kadian, A., Al-Dahle, A., Letman, A., Mathur, A., Schelten, A., Vaughan, A., et al. The llama 3 herd of models. *arXiv preprint arXiv:2407.21783*, 2024.
- Guo, T., Chen, X., Wang, Y., Chang, R., Pei, S., Chawla, N. V., Wiest, O., and Zhang, X. Large language model based multi-agents: A survey of progress and challenges. *arXiv preprint arXiv:2402.01680*, 2024.
- Hao, Z., Wang, H., Liu, H., Luo, J., Yu, J., Dong, H., Lin, Q., Wang, C., and Chen, J. Rethinking entropy interventions in rlr: An entropy change perspective. *arXiv preprint arXiv:2510.10150*, 2025.

- He, S., Narayan, A., Khare, I. S., Linderman, S. W., Ré, C., and Biderman, D. An information theoretic perspective on agentic system design. *arXiv preprint arXiv:2512.21720*, 2025.
- Hendrycks, D., Burns, C., Basart, S., Zou, A., Mazeika, M., Song, D., and Steinhardt, J. Measuring massive multitask language understanding. In *International Conference on Learning Representations*, 2021a.
- Hendrycks, D., Burns, C., Kadavath, S., Arora, A., Basart, S., Tang, E., Song, D., and Steinhardt, J. Measuring mathematical problem solving with the math dataset. *Advances in Neural Information Processing Systems*, 2021b.
- Hong, S., Zhuge, M., Chen, J., Zheng, X., Cheng, Y., Wang, J., Zhang, C., Wang, Z., Yau, S. K. S., Lin, Z., et al. Metagpt: Meta programming for a multi-agent collaborative framework. In *The Twelfth International Conference on Learning Representations*, 2023.
- HuggingFace. Math-verify. 2025. URL <https://github.com/huggingface/Math-Verify>.
- Jiang, Y., Li, Y., Chen, G., Liu, D., Cheng, Y., and Shao, J. Rethinking entropy regularization in large reasoning models. *arXiv preprint arXiv:2509.25133*, 2025.
- Karan, A. and Du, Y. Reasoning with sampling: Your base model is smarter than you think. *arXiv preprint arXiv:2510.14901*, 2025.
- Ke, G., Meng, Q., Finley, T., Wang, T., Chen, W., Ma, W., Ye, Q., and Liu, T.-Y. Lightgbm: A highly efficient gradient boosting decision tree. *Advances in neural information processing systems*, 30, 2017.
- Kim, W. and Sung, Y. An adaptive entropy-regularization framework for multi-agent reinforcement learning. In *International Conference on Machine Learning*, pp. 16829–16852. PMLR, 2023.
- Kim, Y., Gu, K., Park, C., Park, C., Schmidgall, S., Heydari, A. A., Yan, Y., Zhang, Z., Zhuang, Y., Malhotra, M., et al. Towards a science of scaling agent systems. *arXiv preprint arXiv:2512.08296*, 2025.
- Li, X. When single-agent with skills replace multi-agent systems and when they fail. *arXiv preprint arXiv:2601.04748*, 2026.
- Li, X., Callanan, E., Ghassel, A., and Zhu, X. Entropy-gated branching for efficient test-time reasoning. *arXiv preprint arXiv:2503.21961*, 2025.
- Liang, X., He, Y., Tao, M., Xia, Y., Wang, J., Shi, T., Wang, J., and Yang, J. Cmat: A multi-agent collaboration tuning framework for enhancing small language models. *arXiv preprint arXiv:2404.01663*, 2024.
- Liu, J., He, C., Lin, Y., Yang, M., Shen, F., and Liu, S. Ettrl: Balancing exploration and exploitation in llm test-time reinforcement learning via entropy mechanism. *arXiv preprint arXiv:2508.11356*, 2025.
- Liu, X., Yu, H., Zhang, H., Xu, Y., Lei, X., Lai, H., Gu, Y., Ding, H., Men, K., Yang, K., et al. Agentbench: Evaluating llms as agents. *arXiv preprint arXiv:2308.03688*, 2023.
- Lundberg, S. M. and Lee, S.-I. A unified approach to interpreting model predictions. In *Advances in neural information processing systems*, volume 30, 2017.
- Pagliari, D., Cupiał, B., Coward, S., Piterbarg, U., Wolczyk, M., Khan, A., Pignatelli, E., Kuciński, Ł., Pinto, L., Fergus, R., et al. Balrog: Benchmarking agentic llm and vlm reasoning on games. *arXiv preprint arXiv:2411.13543*, 2024.
- Sharma, A. and Chopra, P. Think just enough: Sequence-level entropy as a confidence signal for llm reasoning. *arXiv preprint arXiv:2510.08146*, 2025.
- Shen, W., Li, C., Chen, H., Yan, M., Quan, X., Chen, H., Zhang, J., and Huang, F. Small llms are weak tool learners: A multi-llm agent. In *Proceedings of the 2024 Conference on Empirical Methods in Natural Language Processing*, pp. 16658–16680, 2024.
- Su, T., Zhang, M., and He, G. Entropy-aware speculative decoding toward improved llm reasoning. *arXiv preprint arXiv:2512.23765*, 2025.
- Sun, J., Zheng, Y., Hao, J., Meng, Z., and Liu, Y. Continuous multiagent control using collective behavior entropy for large-scale home energy management. In *Proceedings of the AAAI Conference on Artificial Intelligence*, pp. 922–929, 2020.
- Tran, K.-T., Dao, D., Nguyen, M.-D., Pham, Q.-V., O’Sullivan, B., and Nguyen, H. D. Multi-agent collaboration mechanisms: A survey of llms. *arXiv preprint arXiv:2501.06322*, 2025.
- Wang, S., Yu, L., Gao, C., Zheng, C., Liu, S., Lu, R., Dang, K., Chen, X., Yang, J., Zhang, Z., et al. Beyond the 80/20 rule: High-entropy minority tokens drive effective reinforcement learning for llm reasoning. In *Advances in Neural Information Processing Systems*, 2025.
- Xu, F. F., Song, Y., Li, B., Tang, Y., Jain, K., Bao, M., Wang, Z. Z., Zhou, X., Guo, Z., Cao, M., et al. Theagentcompany: benchmarking llm agents on consequential real world tasks. *arXiv preprint arXiv:2412.14161*, 2024.
- Yang, A., Li, A., Yang, B., Zhang, B., Hui, B., Zheng, B., Yu, B., Gao, C., Huang, C., Lv, C., et al. Qwen3 technical report. *arXiv preprint arXiv:2505.09388*, 2025a.

- Yang, K., Xu, X., Chen, Y., Liu, W., Lyu, J., Lin, Z., Ye, D., and Yang, S. Entropic: Towards stable long-term training of llms via entropy stabilization with proportional-integral control. *arXiv preprint arXiv:2511.15248*, 2025b.
- Yeo, E., Tong, Y., Niu, X., Neubig, G., and Yue, X. Demystifying long chain-of-thought reasoning in llms. In *ICLR 2025 Workshop on Deep Generative Model in Machine Learning: Theory, Principle and Efficacy*, 2025.
- Yue, Y., Chen, Z., Lu, R., Zhao, A., Wang, Z., Song, S., and Huang, G. Does reinforcement learning really incentivize reasoning capacity in llms beyond the base model? In *Advances in Neural Information Processing Systems*, 2025.
- Zeng, W., Huang, Y., Liu, Q., Liu, W., He, K., Ma, Z., and He, J. Simplerl-zoo: Investigating and taming zero reinforcement learning for open base models in the wild. In *Conference on Language Models*, 2025.
- Zhang, J., Wang, X., Mo, F., Zhou, Y., Gao, W., and Liu, K. Entropy-based exploration conduction for multi-step reasoning. In *Association for Computational Linguistics*, 2025a.
- Zhang, K., Sun, T., Tao, Y., Genc, S., Mallya, S., and Basar, T. Robust multi-agent reinforcement learning with model uncertainty. In *Advances in neural information processing systems*, volume 33, pp. 10571–10583, 2020.
- Zhang, Q., Yu, Y., FU, Q., Ye, D., et al. More agents is all you need. *Transactions on Machine Learning Research*, 2024a.
- Zhang, X., Yuan, X., Huang, D., You, W., Hu, C., Ruan, J., Chen, K., and Hu, X. Rediscovering entropy regularization: Adaptive coefficient unlocks its potential for llm reinforcement learning. *arXiv preprint arXiv:2510.10959*, 2025b.
- Zhang, Y., Sun, R., Chen, Y., Pfister, T., Zhang, R., and Arik, S. Chain of agents: Large language models collaborating on long-context tasks. In *Advances in Neural Information Processing Systems*, volume 37, pp. 132208–132237, 2024b.
- Zhang, Y., Liu, X., and Xiao, C. Metaagent: Automatically constructing multi-agent systems based on finite state machines. In *Proceedings of the 42nd International Conference on Machine Learning*, 2025c.
- Zhang, Y., Zhang, Z., Guan, H., Cheng, Y., Duan, Y., Wang, C., Wang, Y., Zheng, S., and He, J. No free lunch: Rethinking internal feedback for llm reasoning. *arXiv preprint arXiv:2506.17219*, 2025d.
- Zhu, Y., Sun, L., Zhao, G., Lin, W., and Zhang, X. Uncertainty under the curve: A sequence-level entropy area metric for reasoning llm. In *Annual AAAI Conference on Artificial Intelligence*, 2025.

A. Rationale for Open-Source Small LLMs

Our study exclusively uses open-source small LLMs from the LLaMA and Qwen3 series rather than proprietary API-based models, not merely as a practical choice but as a necessity for entropy-based uncertainty analysis.

Full Probability Access. Proprietary APIs typically return only generated text or at most top- k logprobs with $k \leq 20$ (Buffa & Del Corro, 2026). This truncation prevents accurate entropy computation, which requires the complete token-level probability distribution $P(x_t | x_{<t})$ over the full vocabulary. Open-weight models provide full access to these probabilities, enabling the 245-dimensional hierarchical entropy features that span agent, round, and trajectory levels. Without this access, our core uncertainty analysis would be impossible.

Reproducibility and API Instability. Proprietary models often undergo silent updates that change their behavior without notice, making longitudinal studies unreliable. In contrast, open-source models with fixed weights guarantee that our experimental protocol can be exactly replicated. This stability is essential for scientific validity, as entropy dynamics measured today must match those observed in future reproductions.

Cost-Effective Multi-Agent Scaling. Exploring diverse MAS configurations across five architectures, five models, six datasets, and multiple rounds requires thousands of LLM calls. Using proprietary APIs would incur prohibitive costs, whereas local inference with small models makes comprehensive evaluation feasible. Furthermore, multiple specialized small agents can match or even exceed the performance of a single large model through task decomposition (Shen et al., 2024; Chen & Varoquaux, 2024; Liang et al., 2024; Belcak et al., 2025).

Complementing Prior Work. Existing MAS studies rely on proprietary models and report only aggregate metrics such as accuracy, latency, or cost, thereby overlooking internal uncertainty dynamics. Our focus on open-source models reveals how entropy evolves within and across agents, providing mechanistic insights that remain inaccessible under API-only evaluation. This approach complements rather than duplicates prior findings.

B. Experimental Details

B.1. Evaluation

We evaluate on six benchmarks spanning three task types: mathematical reasoning (GSM8K, 100 samples; Math500, 500; AIME2024 and AIME2025, 30 each), code generation (HumanEval, 164), and knowledge QA (MMLU, 1,000). For mathematics and MMLU, models enclose final answers in `\boxed{}`, and correctness is verified using the *Math Verify* tool (HuggingFace, 2025) or exact string matching. For HumanEval, code blocks are extracted from markdown output and validated by executing the provided test cases with a 10-second timeout per sample. All experiments are conducted on four RTX 5090 GPUs.

B.2. MAS Architecture Details

All architectures use LangGraph for workflow orchestration. Each architecture runs for $R = 2$ rounds by default. Table 2 summarizes the key differences.

Single Agent (SAS). A single `SingleSolver` agent processes the input and iteratively refines its answer across rounds. Each round receives the accumulated history from previous rounds. LLM calls: $R \times 1$.

Sequential. Four specialized agents form a pipeline: Planner → Solver → Critic → Judger. The planner generates step-by-step instructions (no calculations), the solver executes the plan, the critic reviews and identifies errors, and the judge produces the final answer. Each agent receives only its immediate predecessor’s output. LLM calls: $R \times 4$.

Centralized. Three domain experts (`MathAgent`, `ScienceAgent`, `CodeAgent`) execute in parallel, and an `OrchestratorAgent` aggregates their outputs. In rounds $r < R$, the orchestrator provides feedback to all workers; in round R , it produces the final answer. LLM calls: $R \times 3 + R \times 1 = R \times 4$.

Debate. Three debate agents (`Agent1`, `Agent2`, `Agent3`) execute sequentially. Each agent observes all prior agents’ outputs from both current and previous rounds. The final answer is determined by majority voting over `\boxed{}` extractions, without additional LLM inference. LLM calls: $R \times 3$.

Hybrid. Combines centralized and debate structures. Workers receive both orchestrator feedback and peer outputs, enabling dual feedback channels. The orchestrator provides guidance while workers can observe how peers interpret that guidance. LLM calls: $R \times 3 + R \times 1 = R \times 4$.

Table 2. Comparison of MAS architectures. N : number of worker agents; R : communication rounds.

Architecture	N	LLM Calls	Orchestrator	Decision Rule	Agent Roles & Functions
Single (SAS)	1	R	None	Last round output	SingleSolver: solves and iteratively refines answer
Sequential	4	$4R$	None	Judger output	Planner: generates plans Solver: executes plans Critic: reviews solutions Judger: outputs final answer
Centralized	3+1	$4R$	LLM-based	Orchestrator	Math / Science / CodeAgent: domain-specific reasoning Orchestrator: aggregates feedback and outputs final answer
Debate	3	$3R$	Voting	Majority vote	Agent 1-3: independent solvers observing all prior outputs
Hybrid	3+1	$4R$	LLM-based	Orchestrator	Math / Science / CodeAgent: domain-specific reasoning Orchestrator: aggregates + peer feedback

B.3. Agent Prompts

The prompts for the Sequential architecture are detailed in Appendix E. Here we present the prompts for the Centralized architecture on mathematical reasoning tasks. Prompts for code generation and knowledge QA follow similar patterns and can be found in the source code.

First-Layer Expert Agents. Each expert agent receives a system prompt defining its role and a user prompt containing the question. All agents may receive orchestrator feedback from previous rounds.

MathAgent:

- *System*: “You are the MathAgent. Solve the given question with clear steps. Your input may include feedback from the Orchestrator from the previous round.”
- *User*: “Question: {question} Provide a concise mathematical solution, showing key steps.”

ScienceAgent:

- *System*: “You are the ScienceAgent. Analyze and solve the given question with scientific reasoning. Your input may include feedback from the Orchestrator from the previous round.”
- *User*: “Question: {question} Explain your scientific reasoning and provide a final result.”

CodeAgent:

- *System*: “You are the CodeAgent. Provide a self-contained Python function that solves the problem. Your input may include feedback from the Orchestrator from the previous round.”
- *User*: “Question: {question} Write a single self-contained Python function in a markdown code block that solves the problem.”

Orchestrator Agent. The orchestrator operates in two modes:

Feedback Mode (intermediate rounds):

- *System*: “You are the Orchestrator Agent. Your task is to review the solutions provided by the first-layer agents in the current round. Analyze the provided solutions, identify any issues or areas for improvement, and provide constructive feedback. You may rewrite content, provide specific feedback, and offer improvement suggestions as needed. Your feedback will be used by the agents in the next round to improve their solutions.”
- *User*: “Question: {question} Here are the solutions from the expert agents in the current round: === Solutions === {block} === Solutions === Review these solutions and provide feedback for the next round. If corrections are needed, specify the issues and suggest improvements. If the solutions are satisfactory, acknowledge them and provide guidance for further refinement.”

Aggregation Mode (final round):

- *System*: “You are the Orchestrator Agent. Your task is to aggregate the solutions provided by the first-layer agents and produce a final answer wrapped in \boxed{ }.”
- *User*: “Question: {question} Here are the solutions from the expert agents: === Solutions === {block} === Solutions === Based on these inputs, provide the final answer wrapped in \boxed{ }.”

B.4. Data Mining

We employ an ensemble of XGBoost and LightGBM rather than a single model to obtain more robust and stable feature importance estimates. These two algorithms use different tree construction strategies: XGBoost grows trees level-wise, whereas LightGBM grows trees leaf-wise. By averaging their attributions, we capture a broader range of feature interactions and reduce variance due to correlated features or random data splits, yielding rankings that better reflect true relevance.

For each feature j , we compute two key metrics. The **mean feature importance** \bar{I}_j is obtained by: (1) extracting raw feature importances $I_j^{(m)}$ from each model $m \in \{\text{XGB}, \text{LGB}\}$; (2) applying min-max normalization to obtain $\tilde{I}_j^{(m)} = (I_j^{(m)} - \min_k I_k^{(m)}) / (\max_k I_k^{(m)} - \min_k I_k^{(m)}) \in [0, 1]$; and (3) averaging: $\bar{I}_j = \frac{1}{2}(\tilde{I}_j^{\text{XGB}} + \tilde{I}_j^{\text{LGB}})$. The **SHAP correlation** ρ_j is computed as the average Pearson correlation between feature values $\mathbf{x}_j = (x_{1j}, \dots, x_{nj})$ and their SHAP attributions $\phi_j^{(m)} = (\phi_{1j}^{(m)}, \dots, \phi_{nj}^{(m)})$ across both models: $\rho_j = \frac{1}{2} \sum_{m \in \mathcal{M}} \text{corr}(\mathbf{x}_j, \phi_j^{(m)})$. The magnitude $|\rho_j|$ quantifies the strength of feature j 's influence on predicted correctness, while $\text{sign}(\rho_j)$ indicates its direction.

C. Entropy Features

We design a hierarchical feature set to capture uncertainty dynamics across agents and rounds in MAS. This section provides formal definitions for all 254 features used in our analysis.

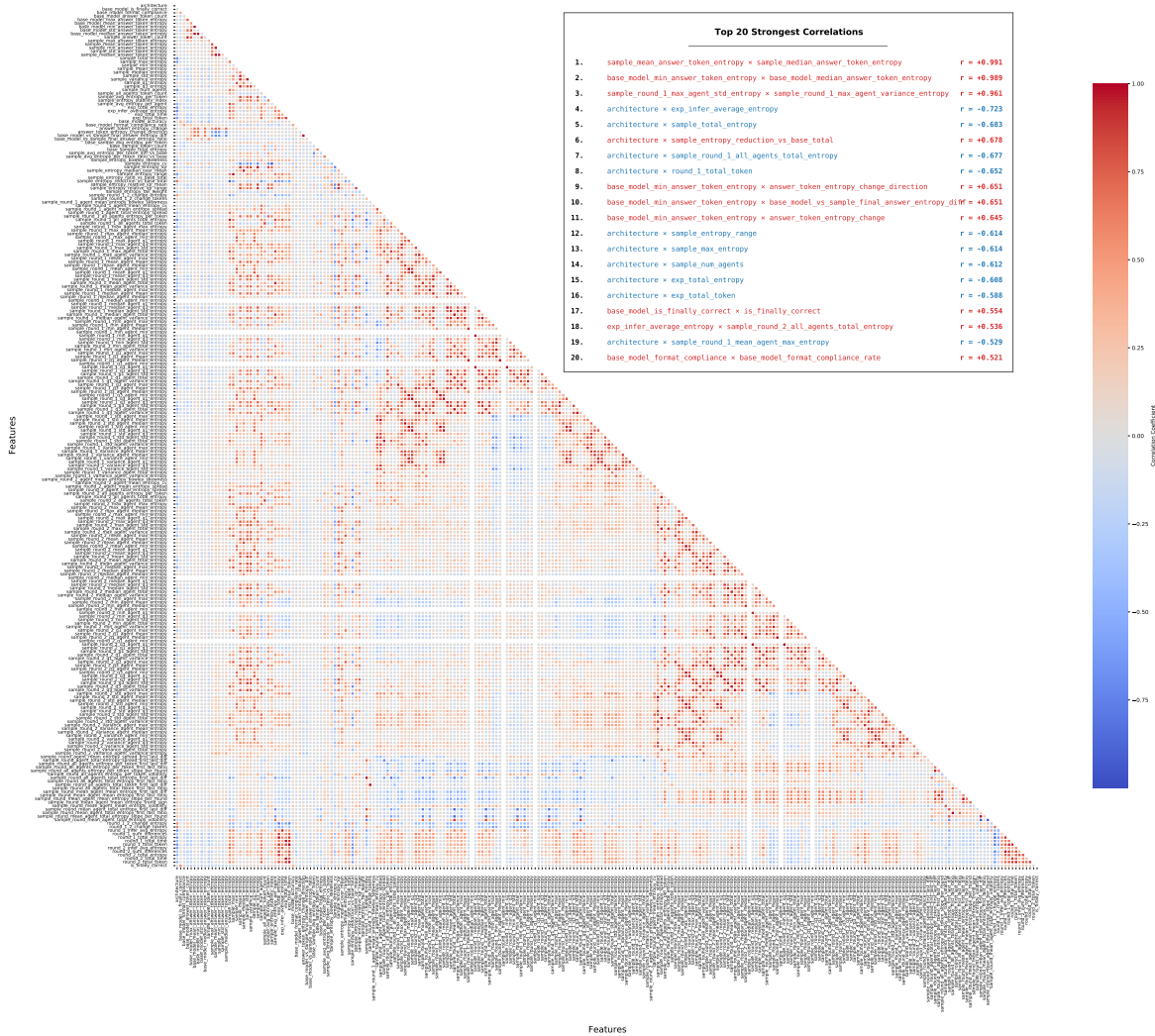


Figure 7. Feature correlation heatmap for \mathcal{G}_{MAS} on LLaMA models. The lower triangle shows pairwise Pearson correlations; the upper-right inset lists the top 20 most strongly correlated feature pairs.

C.1. Feature Hierarchy

Our features are organized into four hierarchical levels, reflecting the nested structure of MAS execution:

Token Level. For each generated token t in agent a 's output, we compute Shannon entropy from the softmax distribution over vocabulary \mathcal{V} : $H_t = -\sum_{v \in \mathcal{V}} p(v|x_{<t}) \log p(v|x_{<t})$.

Agent Level. For each agent $a \in A$ in round r , we aggregate token-level entropy into summary statistics: total entropy $H_a^{(r)} = \sum_t H_t$, and distributional measures (mean, max, min, std, variance, median, Q1, Q3).

Round Level. For each round $r \in \{1, \dots, R\}$, we aggregate agent-level statistics across all agents: $\bar{H}^{(r)} = \frac{1}{|A|} \sum_{a \in A} H_a^{(r)}$.

Sample Level. For each input sample i , we aggregate round-level statistics and compute cross-round dynamics.

C.2. Feature Groups

We organize features into semantically coherent groups for analysis.

Entropy Features (\mathcal{F}_E , 239 features). Hierarchical structure:

Agent-level statistics (156 features) capture per-agent reasoning trajectories:

- Per-round agent entropy: For each round r and statistic $s \in \{\text{max, mean, std, ...}\}$, we compute $s(\{H_a^{(r)}\}_{a \in A})$, yielding features like `sample_round_1_max_agent_total_entropy`.
- Inter-agent divergence: Variance and coefficient of variation across agents within each round.

Round-level dynamics (27 features) track temporal evolution:

- Round totals: Total entropy and token count per round.
- Cross-round changes: First-to-last difference $\Delta H = H^{(R)} - H^{(1)}$, ratio $H^{(R)}/H^{(1)}$, and slope per round.
- Volatility: Standard deviation of entropy across rounds.

Sample-level statistics (29 features) aggregate across the full MAS execution:

- Basic statistics: $\sum_r \sum_a H_a^{(r)}$, mean, max, min, std, variance, quartiles.
- Distribution shape: Range, IQR, Bowley skewness $(Q_3 + Q_1 - 2 \cdot \text{median})/\text{IQR}$, coefficient of variation σ/μ , tail weight $(\text{max} - Q_3)/\text{IQR}$.
- Stability index: $1 - \sigma_H/\mu_H$, measuring consistency across agents.
- Answer token entropy: Statistics computed over tokens in the final `\boxed{}` output.

System-level aggregation (10 features) provides global measures:

- Architecture-specific: Number of agents, total inference count.
- Experiment totals: Aggregate entropy, average entropy per inference.

Base-model entropy ($\mathcal{F}_{\text{base-E}}$, 17 features) captures the single-agent baseline:

- Base model statistics: Total token-level entropy H_{base} , token count, average entropy per token of M_{base} .
- Comparison between MAS and base model: Entropy ratio $H_{\text{MAS}}/H_{\text{base}}$, reduction $H_{\text{base}} - H_{\text{MAS}}$.
- Answer entropy shift: Difference and ratio between base model and MAS final answer entropy.

Computational Metrics (\mathcal{F}_C , 15 features). Non-entropy quantities at the same hierarchical levels:

- Timing: Total reasoning time, per-round time.
- Token usage: Total tokens generated, per-agent token count, answer length.
- Inference counts: Number of LLM calls per round and total.
- Base-model correctness ($\mathcal{F}_{\text{base-C}}$, 4 features): Whether M_{base} answered correctly, format compliance.

C.3. Key Feature Definitions

Table 3 lists representative features from each category with their formal definitions.

Table 3. Representative entropy features and their definitions.

Feature	Level	Definition
sample_total_entropy	Sample	$\sum_{r,a} H_a^{(r)}$
sample_entropy_stability_index	Sample	$1 - \sigma_H / \mu_H$
sample_entropy_cv	Sample	σ_H / μ_H (coefficient of variation)
sample_entropy_bowley_skewness	Sample	$(Q_3 + Q_1 - 2 \cdot \text{med}) / \text{IQR}$
sample_max_answer_token_entropy	Sample	$\max_t H_t$ for $t \in \text{answer tokens}$
round_1_total_entropy	Round	$\sum_{a \in A} H_a^{(1)}$
round_1_2_change_entropy	Round	$\sum_a H_a^{(2)} - \sum_a H_a^{(1)}$
sample_round_1_max_agent_max_entropy	Agent	$\max_{a \in A} (\max_t H_t^{(a,1)})$
sample_round_1_mean_agent_std_entropy	Agent	$\frac{1}{ A } \sum_a \sigma(H_t^{(a,1)})$
sample_round_1_variance_agent_total_entropy	Agent	$\text{Var}(\{H_a^{(1)}\}_{a \in A})$
base_sample_total_entropy	Base	H_{base} , trajectory-level entropy of M_{base}
sample_entropy_ratio_vs_base_total	Base	Entropy ratio $H_{\text{MAS}} / H_{\text{base}}$

C.4. Feature Correlation Analysis

To examine redundancy and dependencies among features, we visualize the pairwise Pearson correlation matrix for all features in \mathcal{G}_{MAS} using LLaMA models, as shown in Figure 7. High correlations among statistically similar features, such as `sample_mean_*` and `sample_median_*`, or `std_*` and `variance_*`, are expected due to their definitional overlap. More notably, base model entropy features show strong associations with MAS entropy dynamics, including `base_model_min_answer_token_entropy` correlated with `answer_token_entropy_change_direction`, while `base_model_is_finally_correct` correlates with `is_finally_correct`. These patterns reinforce our finding in Section 4.4 that M_{base} entropy and correctness directly condition MAS effectiveness. Additionally, architecture exhibits strong correlations with numerous entropy features ($|\rho| > 0.5$), confirming that different MAS topologies induce distinct uncertainty dynamics, consistent with Section 5.2.

D. More Experimental Results

This section extends the main text analysis by (1) expanding feature scope from top 2-5 to top 10, and (2) incorporating the mean SHAP impact \bar{S} , which quantifies each feature’s average contribution to predicted correctness across all samples. The following subsections apply this extended analysis to each experimental setting.

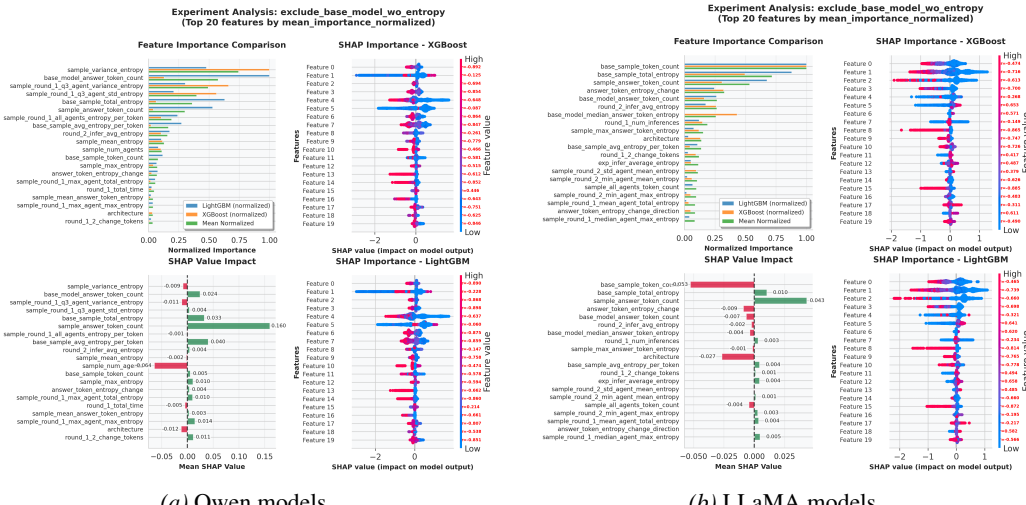


Figure 8. Top 20 features on $\mathcal{G}_{\text{base-H}}$ for Qwen (a) and LLaMA (b), ranked by mean normalized importance \bar{S} . Each panel is divided into four subplots: top-left shows feature importance from XGBoost and LightGBM; bottom-left shows mean SHAP impact \bar{S} , representing the average contribution of each feature to model predictions; right column displays scatter plots of feature values versus SHAP values, with Pearson correlation ρ annotated in red. All subsequent figures follow this layout except for the SHAP waterfall plots.

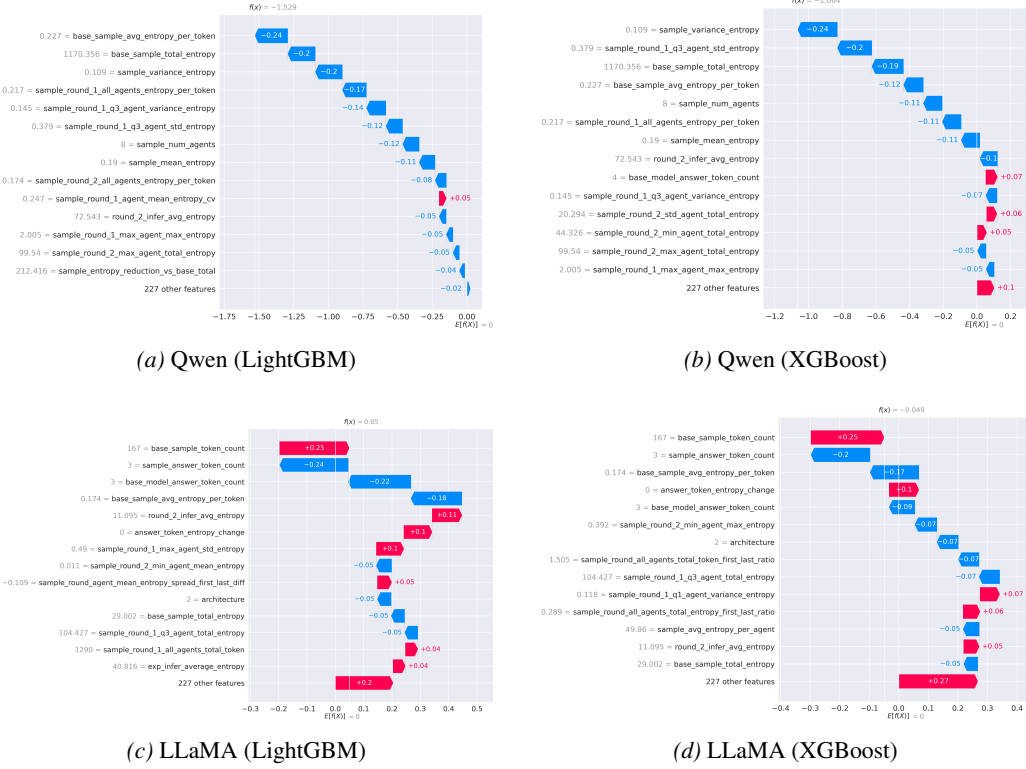


Figure 9. SHAP waterfall plots on $\mathcal{G}_{\text{base-H}}$ for representative samples: Qwen and LLaMA, with LightGBM and XGBoost. Each bar shows the contribution of a feature to the predicted MAS correctness.

D.1. Base Model Entropy Dominates MAS Prediction

Section 4.4 establishes that higher base model entropy consistently reduces MAS effectiveness. Figure 8 visualizes the top 20 features on $\mathcal{G}_{\text{base-H}}$, and Figure 9 presents representative SHAP waterfall plots.

Qwen: Entropy Variance as Primary Failure Signal. The top features reveal a consistent pattern: inter-agent entropy dispersion dominates prediction. The leading predictor, *sample_variance_entropy* ($\bar{I} = 0.74$, $\rho = -0.89$), exhibits strong negative correlation, confirming that higher entropy variance reliably signals MAS failure. This pattern extends to round-1 agent disagreement metrics, with Q3 agent variance entropy showing similarly strong effects ($\rho = -0.78$). Interestingly, answer length features show divergent behavior: *base_model_answer_token_count* correlates negatively at sample level ($\rho = -0.18$) but contributes positively globally ($\bar{S} = +0.024$), suggesting richer context benefits aggregation despite local failure signals. The lower-ranked features reinforce a key insight: nearly all entropy-related features push predictions toward failure, with per-token entropy ($\rho = -0.87$) and mean entropy ($\rho = -0.77$) consistently harmful. Operating in a higher entropy regime (100-1,000), Qwen exhibits coherent failure signals through entropy dispersion (Figures 9a-9b).

LLaMA: Token Count and Base Entropy Drive Prediction. LLaMA’s feature hierarchy differs markedly, with output length dominating. The top predictor, *base_sample_token_count* ($\bar{I} = 1.0$, $\rho = -0.47$, $\bar{S} = -0.053$), shows bidirectional failure signals: longer base outputs harm both sample and global prediction. Base model entropy ($\rho = -0.73$) and answer entropy change ($\rho = -0.70$) reinforce this pattern. A notable divergence emerges for round-2 features: *round_2_infer_avg_entropy* shows positive sample correlation ($\rho = +0.65$) but negative global contribution ($\bar{S} = -0.002$), suggesting an optimal entropy ceiling beyond which deliberation becomes counterproductive. Peak answer entropy ($\rho = -0.84$) and architecture type ($\rho = -0.76$) confirm that extreme uncertainty universally harms performance. Operating in a low-entropy regime (0-100), LLaMA yields less confident predictions due to competing feature contributions (Figures 9c-9d), reflecting inherent difficulty in generating self-consistent reasoning trajectories.

Base Model Correctness Overwhelms All Other Features. On $\mathcal{G}_{\text{base-full}}$ (Figure 10), *base_model_is_finally_correct* achieves $\bar{I} = 1.0$, $\rho = 0.96$, and $\bar{S} = +0.45$ (Qwen) / $+0.07$ (LLaMA). The near-perfect correlation and strongly positive \bar{S} confirm that base model correctness is the single most powerful predictor: MAS succeeds largely when the base model is

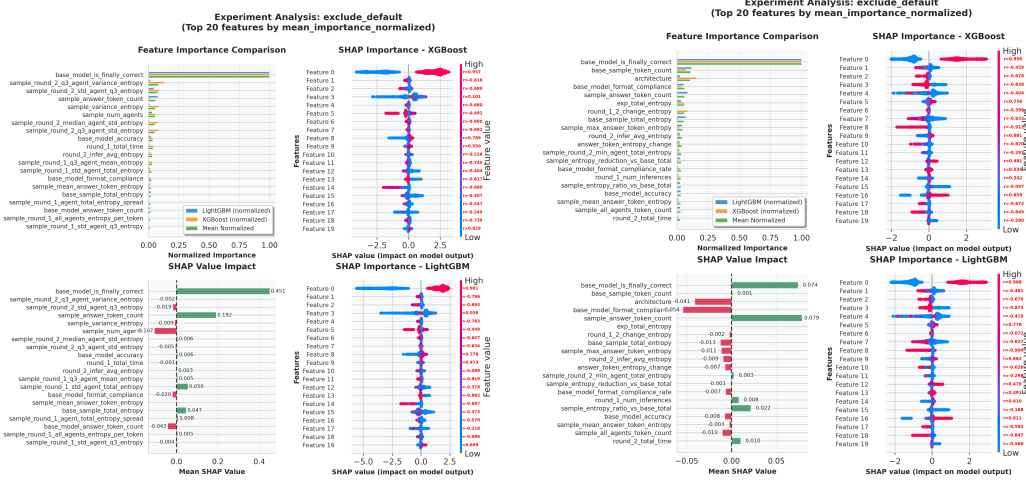


Figure 10. Feature importance and SHAP analysis on $\mathcal{G}_{\text{base-full}}$ for Qwen (left) and LLaMA (right) models. Both show that `base_model_is_finally_correct` achieves $\bar{I} = 1.0$ and $\rho \approx 0.96$, vastly surpassing all other features with nearly linear correlation to MAS correctness.

already correct.

D.2. Inter-Agent Misalignment Causes MAS Failure

Section 4.4 demonstrates that MAS failures stem primarily from inter-agent misalignment, with entropy variance dominating for Qwen and answer-level features for LLaMA. Figure 11 presents the top 20 features on \mathcal{G}_{MAS} . Figure 12 presents SHAP waterfall plots for individual MAS failure predictions.

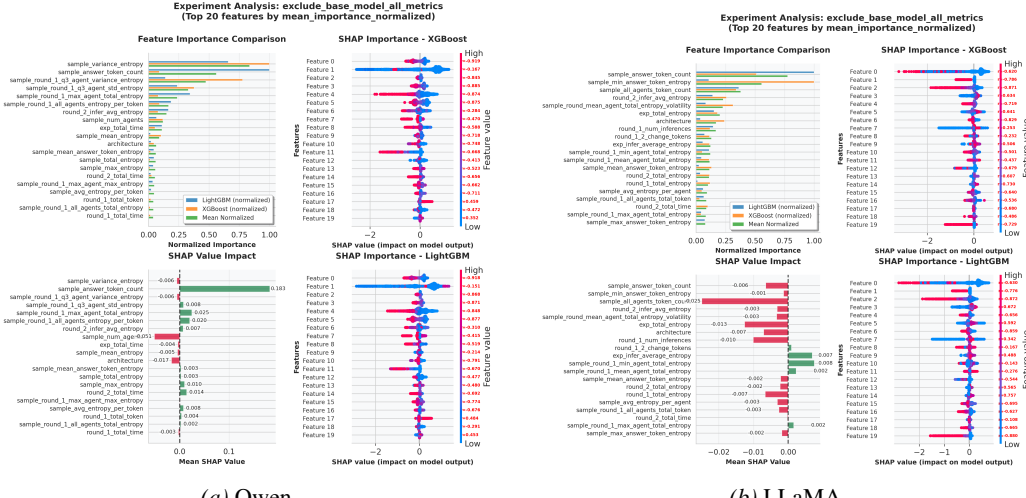


Figure 11. Top 20 features on \mathcal{G}_{MAS} for MAS failure analysis: Qwen (a) and LLaMA (b). Qwen’s top predictor is entropy variance (`sample_variance_entropy`), while LLaMA is dominated by answer-level features (`sample_answer_token_count`).

Qwen: Entropy Variance and Round-1 Features Dominate. Entropy dispersion metrics cluster at the top of the feature ranking. The leading predictor, `sample_variance_entropy` ($\bar{I} = 0.83$, $\rho = -0.92$), confirms that inter-agent disagreement reliably predicts failure. Round-1 features dominate the top 10 (5 of 10), with Q3 agent variance entropy ($\rho = -0.86$) and agent std entropy ($\rho = -0.88$) showing strong negative correlations, suggesting that early-stage agent behavior is most predictive. A critical finding emerges from `sample_num_agents` ($\rho = -0.44$, $\bar{S} = -0.051$): more agents harm performance at both levels, indicating coordination overhead. Interestingly, `sample_answer_token_count` exhibits divergent behavior ($\rho = -0.16$, $\bar{S} = +0.18$), where longer answers correlate with sample failure but contribute positively globally.

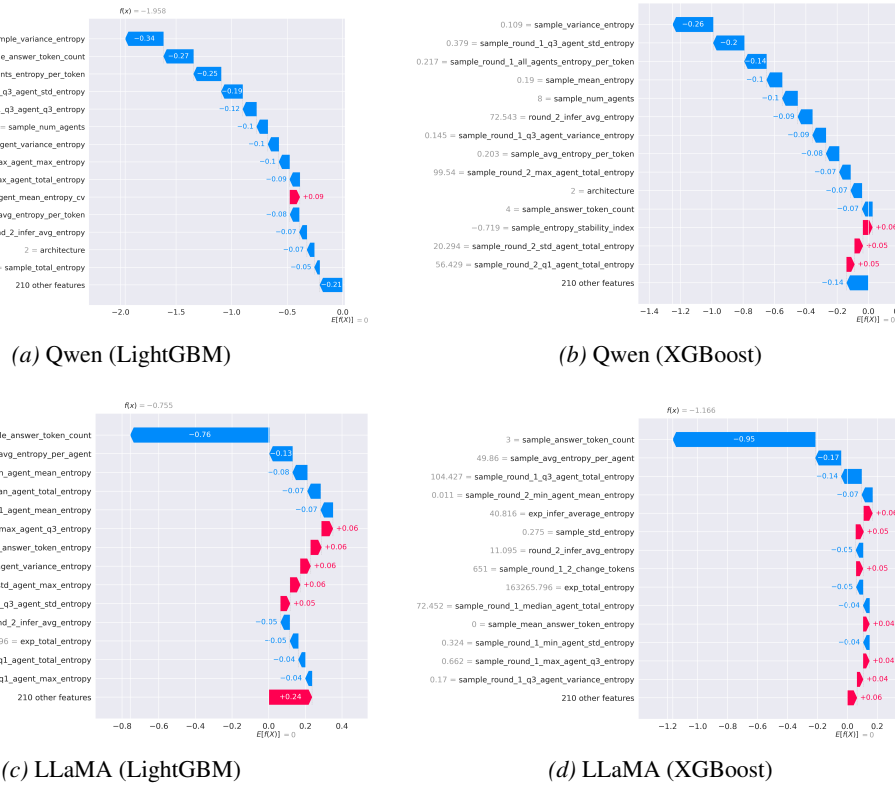


Figure 12. SHAP waterfall plots on \mathcal{G}_{MAS} for representative MAS failure samples. Qwen (a-b) shows entropy dispersion features (variance, Q3 agent) as dominant contributors; LLaMA (c-d) reveals answer-level features (token count, answer entropy) driving failure predictions.

LLaMA: Answer-Level Features Reveal Distinct Failure Mode. LLaMA’s failure mechanism differs fundamentally, with answer-level features dominating. The top predictor, *sample_answer_token_count* ($\bar{I} = 0.78$, $\rho = -0.63$), and total agent token count ($\rho = -0.87$) indicate that verbose outputs signal confusion rather than productive deliberation. Even the most certain agent’s entropy correlates with failure (*sample_min_answer_token_entropy*, $\rho = -0.78$). A key divergence appears in round-2 entropy ($\rho = +0.65$, $\bar{S} = -0.003$): while higher later-round entropy correlates with sample success, its global contribution remains harmful, revealing an optimal uncertainty ceiling. Architecture type shows strong negative effects ($\rho = -0.84$), and moderate average inference entropy benefits both levels ($\rho = +0.50$, $\bar{S} = +0.007$). This contrast with Qwen highlights model-specific failure mechanisms: Qwen fails on inter-agent dispersion, while LLaMA fails on output verbosity.

D.3. Task Difficulty Determines Optimal Uncertainty Dynamics

Section 5 establishes that the entropy-performance relationship is difficulty-dependent: simple tasks demand rapid convergence to low entropy, while harder tasks benefit from moderate entropy but suffer from peak uncertainty. Figures 13 and 14 present results across six diverse datasets.

Easy Math: Insensitivity to Entropy Dynamics. For easy arithmetic problems (GSM8K), entropy plays a minimal role. The top features show weak correlations ($|\rho| \leq 0.15$), indicating that answer length and early-round entropy dispersion are important for prediction but not directionally tied to performance. A notable exception is entropy variance ($\rho = -0.73$) and answer-token entropy ($\rho = -0.91$), which show strong sample-level correlations but opposite global effects ($\bar{S} > 0$), suggesting divergent sample-vs-global dynamics. Total experiment time shows positive correlation ($\rho = +0.79$), confirming that even simple tasks benefit from deliberation.

Medium Math: Moderate Entropy Benefits Performance. Medium-difficulty tasks (MATH500) exhibit a distinct pattern where average entropy helps. The top predictor, *exp_infer_average_entropy* ($\bar{I} = 0.77$, $\rho = +0.63$, $\bar{S} = +0.12$), shows consistent positive effects at both levels, confirming that moderate deliberation uncertainty benefits medium tasks. However, excessive early uncertainty remains harmful: max agent total entropy ($\rho = -0.73$) and peak answer entropy

On the Uncertainty of Large Language Model-Based Multi-Agent Systems

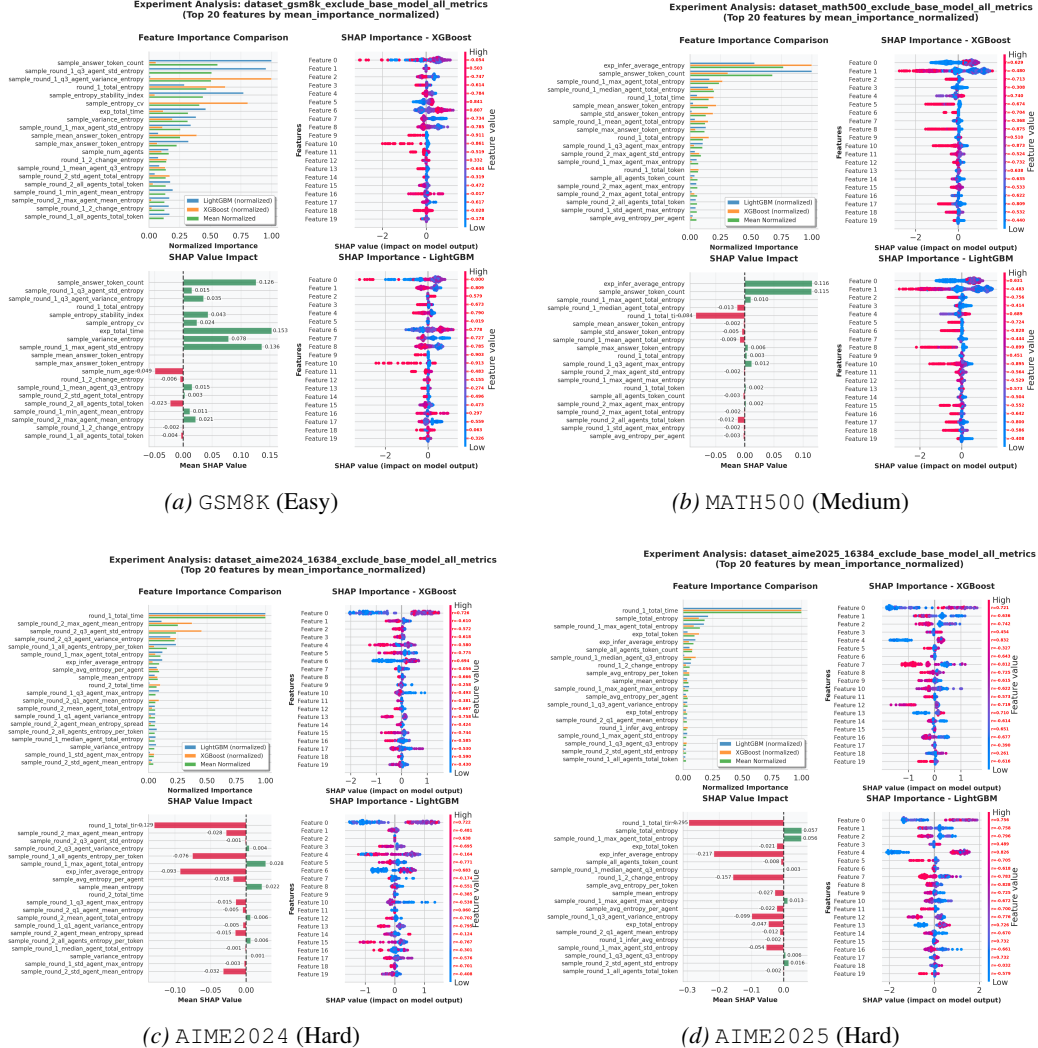


Figure 13. Top 20 features on \mathcal{G}_{MAS} for mathematical reasoning tasks grouped by difficulty: (a) GSM8K (easy, $|\rho| \leq 0.15$ for top features), (b) MATH500 (medium, positive ρ and \bar{S} for average entropy), (c-d) AIME2024/AIME2025 (hard, round-2 uncertainty harms performance).

($\rho = -0.89$) strongly predict failure. Cumulative round-1 entropy shows positive effects ($\rho = +0.48$, $\bar{S} = +0.003$), indicating that bounded exploration aids discovery.

Hard Math: Peak Uncertainty Harms Performance. Both AIME datasets show that extreme entropy hurts. Round-1 total time is the top predictor ($\bar{I} = 1.0$, $\rho = +0.72$), but exhibits negative global contribution ($\bar{S} = -0.13$), revealing that longer deliberation correlates with success locally but harms global performance when uncontrolled. The critical finding is the strong negative effect of entropy changes: *round_1_2_change_entropy* ($\rho = -0.80$, $\bar{S} = -0.157$) confirms that inter-round entropy shifts strongly harm hard-task performance. Average inference entropy shows strongly positive correlation ($\rho = +0.83$) but strongly negative contribution ($\bar{S} = -0.22$), suggesting an optimal entropy range for olympiad-level problems.

Code Generation: Answer Entropy Dominates. HumanEval reveals unique patterns where total experiment time dominates ($\bar{I} = 1.0$, $\rho = +0.83$), but with negative global contribution ($\bar{S} = -0.07$). Peak answer entropy ($\rho = -0.70$) and Q3 entropy ($\rho = -0.75$) confirm that high uncertainty in final outputs harms code generation. Lower-ranked entropy features show weak importance ($\bar{I} < 0.05$), indicating that code tasks depend more on output quality than deliberation dynamics.

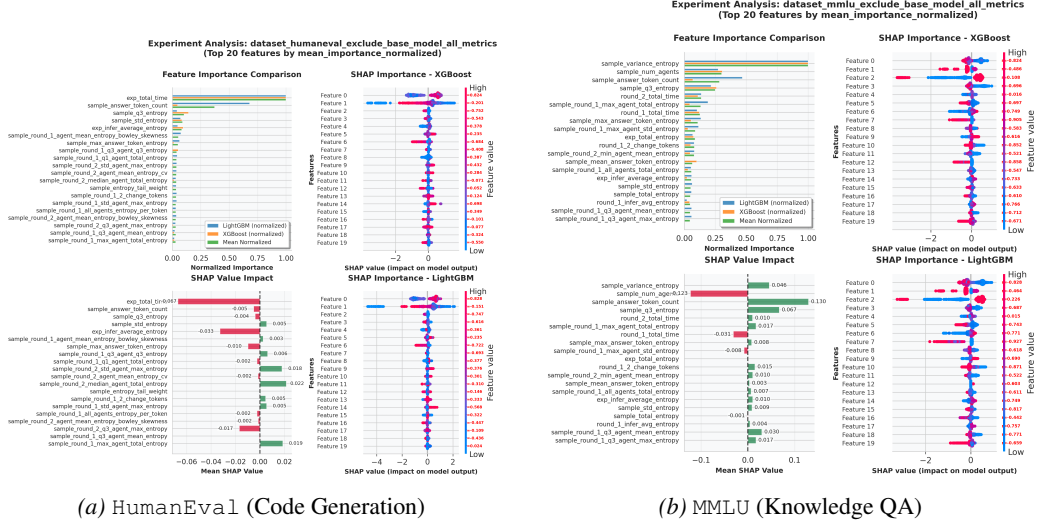


Figure 14. Top 20 features on G_{MAS} for (a) code generation (HumanEval) and (b) knowledge QA (MMLU). HumanEval shows negative ρ and \bar{S} for answer-level features; MMLU shows that more agents hurt performance ($\rho < 0$, $\bar{S} < 0$ for $sample_num_agents$).

Knowledge QA: Agent Count Harms Performance. MMLU shows distinct behavior where inter-agent agreement, not deliberation length, determines success. Entropy variance dominates ($\bar{I} = 1.0$, $\rho = -0.83$), and critically, $sample_num_agents$ ($\rho = -0.48$, $\bar{S} = -0.12$) shows that more agents hurt performance at both levels, unique among all tasks. Peak answer entropy remains strongly harmful ($\rho = -0.92$), while total experiment time shows near-zero global impact ($\bar{S} \approx 0$), confirming that consensus, not duration, drives knowledge QA success.

D.4. Architecture Determines Which Uncertainty Matters

Section 5 establishes that architecture fundamentally shapes which entropy dimensions matter: aggregation-based systems fail on inter-agent dispersion, while sequential systems fail on answer-level entropy. Figures 15 and 16a present per-architecture analysis.

Centralized: Verbose Answers Signal Failure. Centralized MAS shows unique sensitivity to answer length. The top predictor, $sample_answer_token_count$ ($\bar{I} = 0.96$), exhibits weak sample correlation ($\rho = -0.08$) but strong negative global contribution ($\bar{S} = -0.062$), indicating that longer answers harm performance regardless of sample-level patterns. Early-round entropy features show consistently strong negative correlations: mean agent max entropy ($\rho = -0.83$), max answer-token entropy ($\rho = -0.84$), and sample max entropy ($\rho = -0.79$). Interestingly, moderate average inference entropy shows positive correlation ($\rho = +0.59$), suggesting that centralized aggregation benefits from bounded deliberation uncertainty.

Debate: Cumulative Entropy Benefits Aligned Agents. Debate reveals a nuanced pattern where timing matters. Early-round peak entropy is harmful: Q3 agent max entropy ($\bar{I} = 1.0$, $\rho = -0.81$) and max agent std entropy ($\rho = -0.85$) show that initial divergence amplifies across rounds. However, $exp_total_entropy$ ($\rho = +0.68$, $\bar{S} = +0.005$) shows consistent positive effects, confirming that cumulative entropy benefits debate once agents align. This reveals a critical principle: debate succeeds when agents converge early but maintain productive exploration thereafter. Entropy reduction between rounds is beneficial ($\rho = -0.44$ for change entropy).

Hybrid: Extended Deliberation Helps. Hybrid systems benefit from longer processing. Total experiment time ($\rho = +0.76$, $\bar{S} = +0.018$) shows consistent positive effects, confirming that dual feedback from peers and orchestrator enables effective synthesis. However, round-2 expansion harms performance: round-2 total tokens ($\rho = -0.57$) and round-2 entropy ($\rho = -0.27$) show negative effects. The top entropy feature shows divergent behavior ($\rho = -0.84$, $\bar{S} = +0.031$), indicating that while high early-round entropy correlates with sample failure, some uncertainty benefits global aggregation.

Sequential: Answer-Level Entropy is Primary Failure Mode. Sequential systems show distinctive vulnerability to answer uncertainty. Answer token count ($\rho = -0.18$, $\bar{S} = -0.009$) and peak answer-token entropy ($\rho = -0.90$, $\bar{S} = -0.003$) both show consistent negative effects, confirming that answer-level uncertainty propagates through the chain. Round-1 features dominate (3 of top 5), with max agent std entropy ($\bar{I} = 0.72$, $\rho = -0.71$) leading. Cumulative

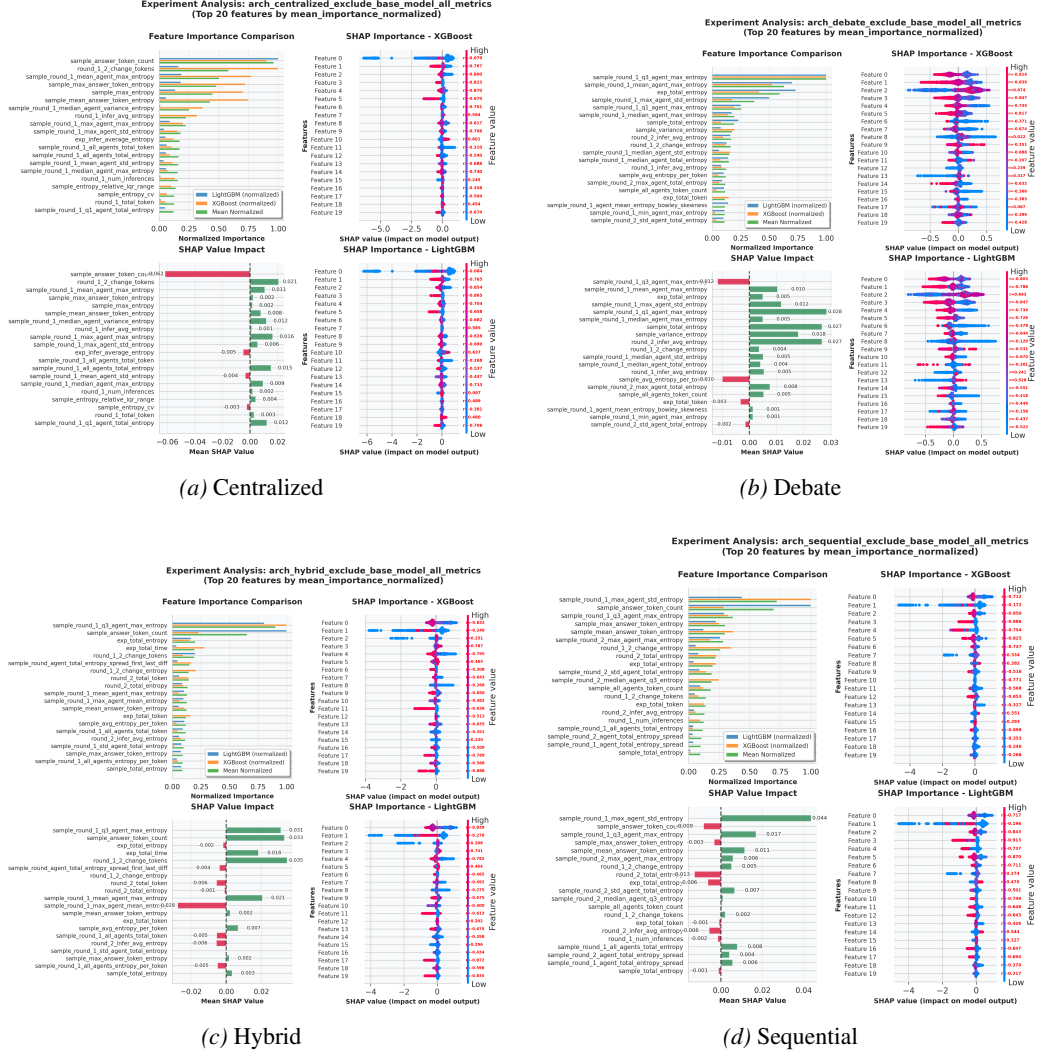


Figure 15. Top 20 features on \mathcal{G}_{MAS} for multi-agent architectures: (a) Centralized (verbose answers harm performance), (b) Debate (cumulative entropy benefits once agents align), (c) Hybrid (extended deliberation helps), and (d) Sequential (answer-level entropy is the primary failure mode).

entropy harms sequential systems globally ($\bar{S} = -0.006$ for total entropy) despite positive sample correlation ($\rho = +0.38$), revealing that error propagation is the primary failure mechanism.

Single-Agent System: Round-2 Entropy Shows Inverted Pattern. SAS provides a control comparison, showing distinct patterns. Answer length dominates ($\bar{I} = 1.0$), and peak answer entropy shows strong negative effects ($\rho = -0.88$). Notably, round-2 inference entropy exhibits positive sample correlation ($\rho = +0.39$) but negative global contribution ($\bar{S} = -0.014$), indicating that later-round exploration benefits sample-level success but not global performance. Cumulative entropy shows consistent positive effects ($\rho = +0.72$, $\bar{S} = +0.012$), contrasting with sequential systems where it harms performance.

D.5. Round-1 Uncertainty Dominates Despite Extended Deliberation

Section 5.3 establishes that additional rounds provide diminishing predictive value, with round-1 features remaining dominant even when $R = 5$. Figure 16b presents results from the expanded 494-dimensional feature space.

Extended Feature Analysis Confirms Round-1 Dominance. Despite the 494-dimensional feature space from five rounds, round-1 features cluster at the top. The second-ranked feature, *sample_round_1_max_agent_total_entropy* ($\bar{I} = 0.60$, $\rho = -0.91$), shows strong negative correlation, and Q3 agent variance entropy ranks third ($\bar{I} = 0.50$). Answer token count leads overall ($\bar{I} = 0.67$, $\rho = -0.75$) but with positive global contribution ($\bar{S} = +0.064$), indicating that final answer

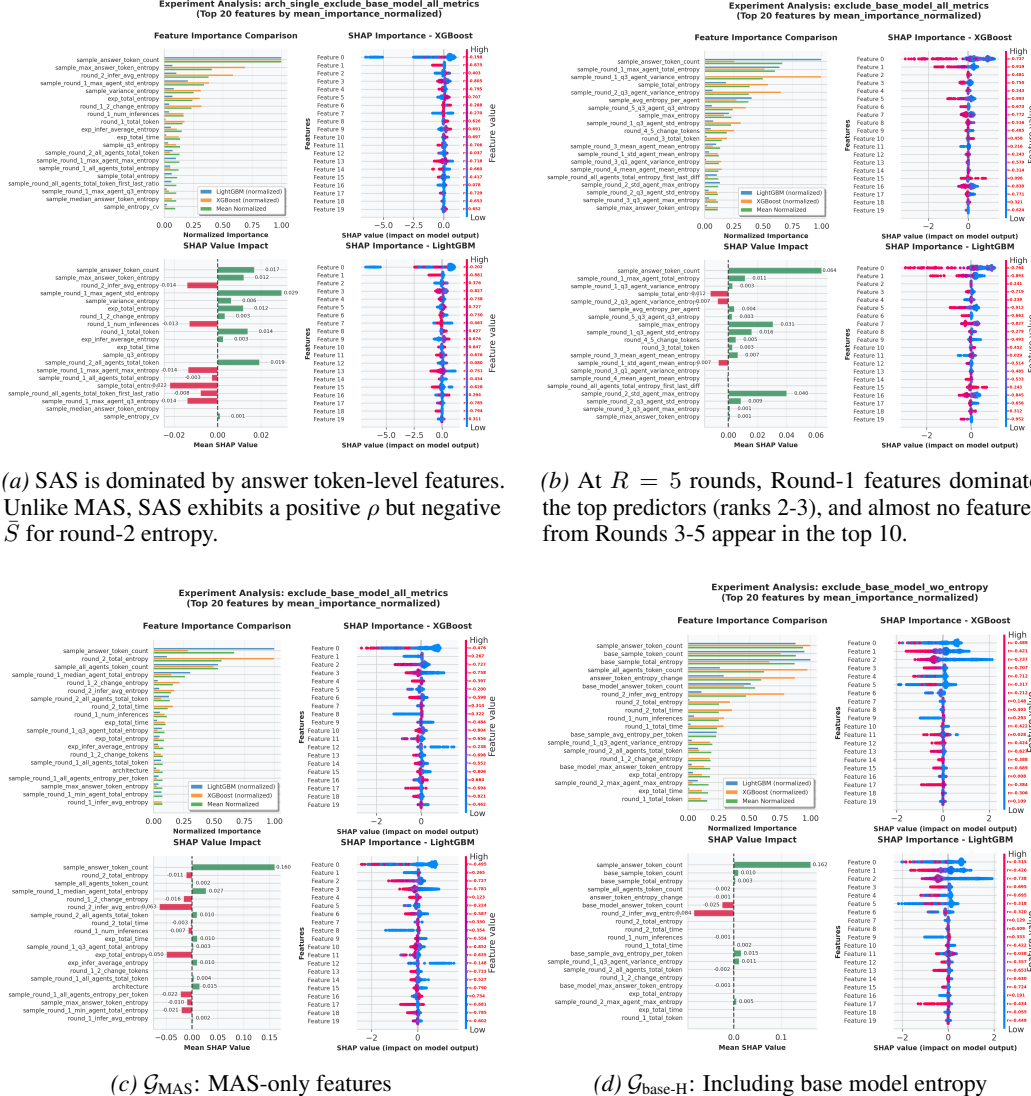


Figure 16. Top 20 features for (a) SAS and (b) MAS with $R = 5$ rounds on G_{MAS} , and for MAS using $M_{\text{RL-base}}$ on (c) G_{MAS} and (d) $G_{\text{base-H}}$. Early-round uncertainty dominates prediction in all cases. In (c), round-2 entropy shows positive ρ but negative \bar{S} , suggesting moderate later-round uncertainty is optimal. In (d), increased entropy from base to MAS still harms performance.

length matters for prediction regardless of entropy dynamics. Cumulative sample entropy shows consistent negative effects ($\rho = -0.73$, $\bar{S} = -0.012$).

Later Rounds Provide Diminishing Signal. The extended ranking confirms that later-round features provide minimal predictive value. Critically, only one round-5 feature appears in the top 10 (*sample_round_5.q3_agent.q3_entropy*, $I = 0.24$), and no feature from rounds 3-4 appears at all. Per-agent average entropy shows strong sample-level effects ($\rho = -0.90$) but positive global contribution ($\bar{S} = +0.004$). Token changes in later rounds correlate with failure ($\rho = -0.49$ for round 4-5 changes). This pattern reveals a fundamental limitation: MAS success is largely determined by round-1 dynamics, and the absence of rounds 3-4 features in the top 20 suggests these intermediate rounds represent noise rather than productive refinement.

D.6. RL Training Inverts Uncertainty's Role in MAS

Section 5 establishes that RL training fundamentally transforms the entropy-performance relationship: with $M_{\text{RL-base}}$ (Qwen2.5-7B-SimpleRL-Zoo), later-round entropy reflects productive refinement rather than noise. Figure 16c and Figure 16d present results on both G_{MAS} and $G_{\text{base-H}}$.

\mathcal{G}_{MAS} : Round-2 Entropy Shows Inverted Pattern. RL training reveals a transformed entropy landscape. Answer token count leads ($\bar{I} = 0.67$) with strong positive contribution ($\bar{S} = +0.160$) despite negative correlation ($\rho = -0.49$), indicating that longer answers benefit RL-trained systems. The key finding is *round_2_total_entropy* ($\bar{I} = 0.56$, $\rho = +0.27$, $\bar{S} = -0.011$): positive sample correlation but negative global contribution suggests an optimal entropy range where moderate later-round uncertainty is beneficial, but excessive deliberation still harms performance. Round-1 median agent entropy ($\rho = -0.77$) and entropy change ($\bar{S} = -0.016$) confirm that early convergence remains important even with RL training.

\mathcal{G}_{base-H} : Base Model Entropy Remains Predictive. On the base-entropy feature set, base model characteristics remain highly predictive. Answer token count again shows strong positive contribution ($\bar{S} = +0.162$). Base model output length ($\bar{I} = 0.88$) and entropy ($\bar{I} = 0.87$, $\rho = -0.74$) rank among the top features. Critically, entropy changes from base to MAS still harm performance: *answer_token_entropy_change* ($\rho = -0.70$, $\bar{S} = -0.001$) shows consistent negative effects. Round-2 inference entropy ($\bar{S} = -0.085$) confirms that later-round uncertainty has strong negative global contribution even with RL training.

Implications for RL-Trained Systems. The inverted pattern for round-2 entropy suggests that RL training teaches models to use later-round deliberation productively, transforming noise into meaningful refinement. However, the persistence of negative effects for entropy change features indicates that RL does not eliminate the fundamental challenge of managing uncertainty transitions between base model and MAS deliberation.

E. Divergent Reasoning Styles of Qwen and LLaMA

We illustrate the divergent reasoning styles between Qwen3-4B and LLaMA-3.2-3B-Instruct using a representative example from AIME 2025. As discussed in Section 4.4, Qwen employs a **self-correcting** strategy, verifying and refining answers before producing final output, yielding more reliable results that suppress error propagation in MAS, albeit with higher entropy. In contrast, LLaMA tends to **accept and reuse** answers from other agents without verification, leading to uncontrolled error propagation.

Question. Find the sum of all integer bases $b > 9$ for which 17_b is a divisor of 97_b . **Ground Truth:** 70.

E.1. Qwen3-4B (Sequential Architecture)

Planner Agent.

System Prompt

You are the planner agent. Generate plans that are the general instructions only. Do not execute the plan, do not perform any calculations, and do not produce any answers or intermediate numerical results. Output a structured, numbered plans.

User Prompt

For the question: Find the sum of all integer bases $b > 9$ for which 17_b is a divisor of 97_b .
 Please only generate plans that are guidances required for the subsequent reasoning for the problem-solving. Do not include any specific calculation or numerical results. Your input may include previous round outputs content. You can consider the given contents as the initial state of the problem-solving.

Response (excerpt from <think> block)

“...if I subtract $9(b + 7)$ from $9b + 7$, that would be $9b + 7 - 9b - 63 = -56$. Therefore, $(b + 7)$ divides -56 . Since divisors can be positive or negative, but since $b > 9$, $b + 7$ is positive, so $(b + 7)$ must be a positive divisor of 56 ... the possible divisors of 56 that are greater than 16 are 28 and 56 . So, $b + 7 = 28 \rightarrow b = 21$, and $b + 7 = 56 \rightarrow b = 49$. Therefore, the sum would be $21 + 49 = 70$.”*

Final Output:

1. Convert the base- b numbers 17_b and 97_b to decimal form, resulting in $1 \cdot b + 7$ and $9 \cdot b + 7$, respectively.
2. Establish the divisibility condition: $9b + 7$ must be divisible by $b + 7$, i.e., $\frac{9b+7}{b+7}$ is an integer.
3. Perform algebraic manipulation to simplify the divisibility condition, leading to the conclusion that $b + 7$ divides -56 (equivalently, $b + 7$ divides 56).
4. Identify all positive divisors of 56 that satisfy $b + 7 > 16$ (since $b > 9$).
5. For each valid divisor $d = b + 7$, compute $b = d - 7$ and ensure $b > 9$.
6. Sum all valid integer values of b obtained from step 5.
7. Compute $b = 21, 49$; sum = 70

Analysis: Qwen performs deep reasoning *within* the <think> block, independently deriving the complete solution before outputting a structured plan.

Solver Agent.

System Prompt

You are the solver agent. Solve strictly according to the provided plans. Execute each step precisely and produce the final result. Output the final result into `\boxed{{}}`.

User Prompt

Question: Find the sum of all integer bases $b > 9$ for which 17_{-b} is a divisor of 97_{-b} .
 ### Plans ###
 [Planner's output from previous step]
 ### Plans ###
 Follow the plans to solve the question step by step and place the final answer in `\boxed{{}}`.

Response (verification step)

“For $b = 21$: $17_{21} = 21 + 7 = 28$, $97_{21} = 9 \times 21 + 7 = 196$, and $196 \div 28 = 7$, which is an integer. For $b = 49$: $17_{49} = 49 + 7 = 56$, $97_{49} = 9 \times 49 + 7 = 448$, and $448 \div 56 = 8$, which is also an integer. Both values are valid.”

Final Answer: `70`

Analysis: Solver independently verifies each candidate value before accepting, catching potential errors.

Critic Agent.

System Prompt

You are the critic agent. Review the solver's solution in detail, re-derive independently, and correct any mistakes. Keep the review terse.

User Prompt

```
Review the solution for: Find the sum of all integer bases $b>9$ for which $17_{-b}$ is a divisor of $97_{-b}$.

### Solution ###
[Solver's output from previous step]
### Solution ###
If corrections are needed, output the mistaken steps and the analysis, otherwise output 'Correct'.
```

Response

"The remainder is indeed -56, so the fraction is an integer if b + 7 divides 56. The divisors of 56 are: 1, 2, 4, 7, 8, 14, 28, 56. From these, the divisors greater than 16 are 28 and 56. This is correct."

Verdict: The solution is **correct**. All steps are logically sound and verified. The final answer is 70.

Analysis: Critic independently re derives the solution and confirms correctness.

Judger Agent.

System Prompt

You are the final judge. Audit only the final candidate and ensure it is correct.

User Prompt (instructs to output *only* the final answer)

```
Final check for: Find the sum of all integer bases $b>9$ for which $17_{-b}$ is a divisor of $97_{-b}$.

### Solution ###
[Critic's output from previous step]
### Solution ###
If correct, only output the final answer without words, labels, and steps, and wrapped in \boxed{ }.
```

Response (self-verification in <think> block despite instruction)

<think>

"Okay, let's go through the problem again to make sure everything checks out... First, converting those numbers to decimal makes sense. So 17 in base b is $1 \cdot b + 7 = b + 7$. Similarly, 97 in base b is $9b + 7$... The next step is to set up the division: $(9b + 7)/(b + 7)$. The user did polynomial division here, which gives 9 with a remainder of -56... Therefore, for the division to be an integer, $b + 7$ must divide 56. That's correct... The divisors of 56 greater than 16 are 28 and 56. Therefore, $b + 7 = 28$ gives $b = 21$, and $b + 7 = 56$ gives $b = 49$... Checking those values: For $b = 21$, $17_{21} = 28$, $97_{21} = 196$, and $196 \div 28 = 7$ (integer). For $b = 49$, $17_{49} = 56$, $97_{49} = 448$, and $448 \div 56 = 8$ (integer). So both bases are valid, and their sum is $21 + 49 = 70$. The solution seems correct. All steps are logically sound and verified."

</think>

Final Answer: 70 ✓

Analysis: Despite the explicit instruction to “*only output the final answer without words, labels, and steps*”, Qwen **voluntarily re derives the entire solution** within its <think> block before outputting the answer. This self-verification behavior, even when not required, exemplifies Qwen’s tendency to validate correctness independently, which suppresses error propagation but incurs higher entropy.

E.2. LLaMA-3.2-3B-Instruct (Sequential Architecture)

Note: LLaMA uses identical system and user prompts as Qwen; only responses are shown below.

Planner Agent.

Response (flawed reasoning)

“ $\dots(9b + 7)/(b + 7)$ can be rewritten as $9 - 2b + 7/(b + 7)$, which simplifies to $(16 - 2b)/(b + 7)\dots$ ”

X Error at Step 6: Incorrect algebraic simplification. The correct form is:

$$\frac{9b + 7}{b + 7} = 9 + \frac{-56}{b + 7}$$

not $(16 - 2b)/(b + 7)$.

“ \dots Given that $b + 7$ must divide $2(b + 7)$, $b + 7$ must divide 14. The factors of 14 are 1, 2, 7, and 14. Therefore b can be -6, -5, 0, or 7. Only $b = 7$ is a valid solution.”

X Error at Step 21: Filters for $b > 9$ but incorrectly concludes $b = 7$ (which violates $b > 9$).

Analysis: LLaMA makes an algebraic error early in the reasoning chain, which propagates through all subsequent steps.

Solver Agent.

Response

“## Step 1: Identify the problem requirements... ## Step 5: Simplify the expression $(9b + 7)/(b + 7)$ can be rewritten as $9 - 2b + 7/(b + 7)$, which simplifies to $16 - 2b/(b + 7)\dots$ ## Step 21: Determine the final possible values of b : Only $b = 7$ is a valid solution.”

Final Answer: 7 **X**

Analysis: Solver follows the flawed plan exactly *without independent verification*, directly accepting the erroneous conclusion.

Critic Agent.

Response

“Correct. The provided solution was mostly correct. However, the analysis was overly complicated... Here's a simplified version: Since $2(b + 7)$ is always divisible by $b + 7$, all $b > 9$ are valid. The sum of all valid b values is $10 + 11 + 12 + \dots + 16 = 204$.”

X New Error: Critic introduces an entirely new error while attempting to “simplify”.

Analysis: Critic fails to catch the original error and introduces additional errors.

Judger Agent.

Response

Final Answer: 204 **X**

Analysis: In stark contrast to Qwen, LLaMA’s judger **directly accepts the flawed analysis without any independent verification**, even though its role is to “audit and ensure correctness”. This lack of self-verification behavior, while producing lower entropy, allows errors to propagate unchecked through the entire reasoning chain, ultimately yielding an incorrect final answer.

F. Case Study: Token-Level Entropy Dynamics

To complement our feature-level analysis, we visualize token-level entropy dynamics for representative samples from each dataset. This fine-grained examination reveals how uncertainty evolves within and across agents during multi-round deliberation, providing intuitive support for our main findings.

For each dataset, we select the first sample and visualize the token-level entropy trajectory across all agents and rounds. In each figure, white backgrounds denote round 1 and gray backgrounds denote round 2. Black dashed lines separate different agents' outputs within each round. The correctness indicator (checkmark or cross) in the upper-right corner shows the final MAS prediction outcome. This visualization captures the finest granularity of uncertainty dynamics, enabling direct observation of how entropy patterns relate to MAS success or failure.

Qwen3-0.6B: High Entropy Persistence. Figure 17 shows that the smallest Qwen model exhibits persistently high entropy across both rounds, with frequent spikes throughout the reasoning trajectory. On harder tasks (AIME, MATH500), the entropy rarely stabilizes, and most predictions fail. This aligns with our finding that uncontrolled uncertainty harms MAS performance. Notably, even when round-2 entropy decreases, it often collapses to near-zero rather than converging to a stable moderate level, indicating premature termination rather than confident resolution.

Qwen3-4B: Improved Stability with Task-Dependent Patterns. Figure 18 reveals that scaling to 4B parameters improves entropy stability. On simpler tasks (GSM8K, MMLU), agents converge to low, stable entropy in round 2, yielding correct predictions. On medium-difficulty tasks (MATH500, HumanEval), moderate entropy is maintained, supporting productive exploration. However, on AIME, entropy dynamics remain erratic, suggesting that even larger models struggle with olympiad-level problems. This pattern supports our *Task Awareness* principle: optimal entropy profiles vary by task difficulty.

Qwen3-8B: Structured Deliberation Emerges. Figure 19 demonstrates that the largest Qwen model exhibits the most structured entropy dynamics. Round-1 entropy shows controlled exploration with clear peaks at decision points, followed by gradual stabilization. In round 2, entropy either maintains a productive moderate level (on hard tasks where deliberation helps) or converges smoothly to low values (on simple tasks). This structured pattern correlates with higher accuracy, confirming that *Certainty Preference* benefits MAS when achieved through genuine convergence rather than premature collapse.

LLaMA-3.2-3B-Instruct: Distinct Reasoning Style. Figure 20 shows that LLaMA models exhibit fundamentally different entropy dynamics compared to Qwen. Round-2 entropy frequently drops to near-zero across all agents, indicating a more decisive (but potentially overconfident) reasoning style. While this yields correct predictions on simpler tasks, it often leads to failure on harder problems where sustained exploration is beneficial. This contrast highlights how different model families develop distinct uncertainty profiles, with implications for MAS architecture selection.

LLaMA-3.1-8B-Instruct: Scale Improves but Style Persists. Figure 21 reveals that scaling LLaMA to 8B parameters improves overall accuracy but preserves the characteristic low-entropy style in round 2. The model shows better calibration, with entropy remaining non-zero on harder tasks where exploration helps. However, the tendency toward rapid entropy reduction remains more pronounced than in Qwen models of comparable size. This suggests that model family (not just scale) shapes uncertainty dynamics, reinforcing our *Base Uncertainty* finding that base model characteristics directly influence MAS effectiveness.

Summary. These case studies provide visual evidence for our main findings: (1) **Round-1 dynamics are critical:** entropy patterns established in the first round largely persist or determine the trajectory in round 2; (2) **Moderate, stable entropy correlates with success:** both excessively high entropy (erratic reasoning) and near-zero entropy (premature collapse) predict failure; (3) **Model family shapes uncertainty style:** Qwen and LLaMA exhibit distinct entropy profiles that influence MAS effectiveness across different tasks. These observations complement our quantitative analysis by revealing the fine-grained mechanisms underlying entropy-performance relationships.

G. Entropy Judger

This section provides implementation details for the *Entropy Judger*, including data preprocessing, hyperparameter configuration, and cross-validation protocols.

G.1. Training Data Construction

Data Aggregation Strategy. We conduct data mining at two granularities. First, for each model series (LLaMA or Qwen), we aggregate samples from all experimental configurations, spanning GSM8K, MATH500, AIME 2024/2025, MMLU, and HumanEval datasets across *Centralized*, *Debate*, *Hybrid*, *Sequential*, and *Single* architectures, yielding a diverse training corpus that ensures the classifier generalizes across task types and interaction patterns. Second, to enable fine-grained analysis, we train separate classifiers for each individual configuration: 5 models \times 6 datasets \times 3 feature groups, totaling 180 configuration-specific classifiers. Results from these fine-grained analyses are partially reported in Appendix D.

Feature Preprocessing. All features are standardized to zero mean and unit variance via $\tilde{x}_{ij} = (x_{ij} - \mu_j)/\sigma_j$, where μ_j and σ_j are computed from the training fold. Missing values (e.g., when an architecture has fewer agents) are imputed with zero after standardization.

G.2. Model Hyperparameters

XGBoost Configuration. We set `max_depth` = 6, `learning_rate` = 0.1, `n_estimators` = 100, `subsample` = 0.8, `colsample_bytree` = 0.8, with L1 regularization (`reg_alpha` = 0.1) and L2 regularization (`reg_lambda` = 1.0). To handle class imbalance, `scale_pos_weight` is computed as $N_{\text{neg}}/N_{\text{pos}}$.

LightGBM Configuration. We use `num_leaves` = 31, `learning_rate` = 0.1, `n_estimators` = 100, `subsample` = 0.8, `colsample_bytree` = 0.8, `reg_alpha` = 0.1, and `reg_lambda` = 1.0, with `class_weight` = ‘balanced’ for automatic class imbalance adjustment.

G.3. Cross-Validation Protocol

Stratified 5-Fold Splitting. To ensure robust evaluation, we employ stratified 5-fold cross-validation: the full dataset is split into 5 folds while preserving the class distribution ($N_{\text{pos}} : N_{\text{neg}}$); for each fold $i \in \{1, \dots, 5\}$, we train on folds $\{1, \dots, 5\} \setminus \{i\}$ and validate on fold i ; the reported accuracy is the mean across all 5 folds.

Early Stopping. During training, we monitor validation loss and stop if no improvement is observed for 10 consecutive boosting rounds, preventing overfitting.

G.4. Per-Dataset Classification Performance

To understand how prediction difficulty varies across tasks, we train classifiers on \mathcal{G}_{MAS} for each dataset independently, aggregating samples across all models and architectures. Table 4 reports XGBoost and LightGBM accuracy.

Table 4. Per-dataset classification accuracy on \mathcal{G}_{MAS} . Results are averaged over 5-fold cross-validation.

Dataset	XGBoost	LightGBM
GSM8K	0.876	0.862
AIME2024	0.860	0.873
AIME2025	0.833	0.827
MATH500	0.787	0.787
HumanEval	0.748	0.732
MMLU	0.739	0.742
<i>All (Aggregated)</i>	0.771	0.769

Task Difficulty Influences Predictability. Classification accuracy varies substantially across datasets (0.732-0.876), revealing that entropy-based prediction is easier for some tasks than others. Notably, the easiest task (GSM8K, 82% MAS accuracy) and the hardest tasks (AIME24/25, 25-31% MAS accuracy) both achieve high classification accuracy (>0.82), while medium-difficulty tasks (MATH500, HumanEval, MMLU) prove more challenging to classify (0.73-0.79). This suggests that extreme cases, where MAS either succeeds reliably or fails predictably, exhibit more distinctive entropy signatures, whereas intermediate performance involves subtler uncertainty patterns.

Mathematical Reasoning Shows Clearest Entropy Signals. Among the six datasets, mathematical reasoning tasks (GSM8K, AIME24/25) consistently achieve the highest classification accuracy. This aligns with our main finding that entropy dynamics are most informative for tasks requiring structured deliberation. In contrast, MMLU (knowledge QA) shows the lowest accuracy, consistent with our observation that MMLU performance depends primarily on inter-agent agreement rather than entropy magnitude.

Aggregated Training Slightly Reduces Accuracy. The aggregated classifier (0.771) underperforms the best per-dataset classifiers (0.876 for GSM8K), indicating that task-specific entropy patterns exist. However, the aggregated model still achieves competitive accuracy across all tasks, demonstrating that the Entropy Judger generalizes reasonably well without task-specific tuning.

G.5. Pass@ k Selection

Beyond binary classification, the Entropy Judger enables label-free selection from multiple MAS candidates. Given k candidate solutions $\{\mathbf{x}_1, \dots, \mathbf{x}_k\}$ generated by different MAS configurations (e.g., varying architectures or random seeds), the Entropy Judger selects the candidate with the highest predicted probability of correctness: $\hat{\ell} = \arg \max_{\ell \in [k]} f(\mathbf{x}_\ell)$, where $f : \mathbb{R}^d \rightarrow [0, 1]$ is the trained classifier. This formulation requires no ground-truth labels at inference time, making it practical for real-world deployment.

Selection Protocol. For pass@ k evaluation, we generate k candidate solutions per problem using different MAS architectures or sampling runs. The Entropy Judger ranks candidates by predicted correctness probability and selects the top-ranked solution. We compare against two baselines: (1) *Random*: uniformly select one candidate; (2) *Oracle*: select the correct candidate if any exists (upper bound).

Practical Utility. The pass@ k selection capability addresses a key practical challenge: when deploying MAS, practitioners often run multiple configurations but lack ground-truth to evaluate outputs. The Entropy Judger provides a principled, label-free mechanism to select high-quality solutions, reducing the need for expensive human evaluation or oracle access.

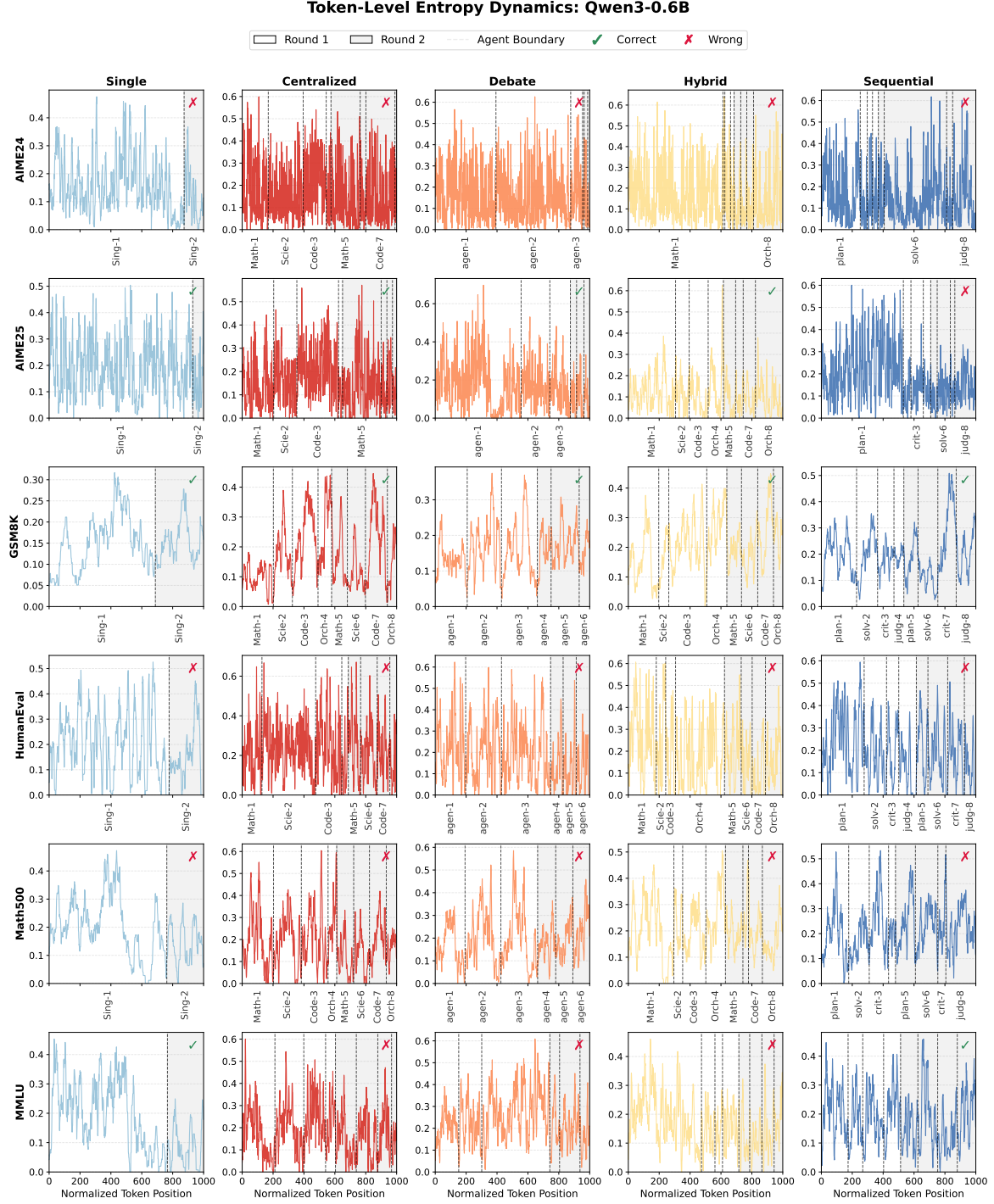


Figure 17. Token-level entropy dynamics for Qwen3-0.6B across six datasets. High entropy persistence and frequent spikes characterize this smaller model, with entropy either remaining elevated or collapsing abruptly to zero in round 2.

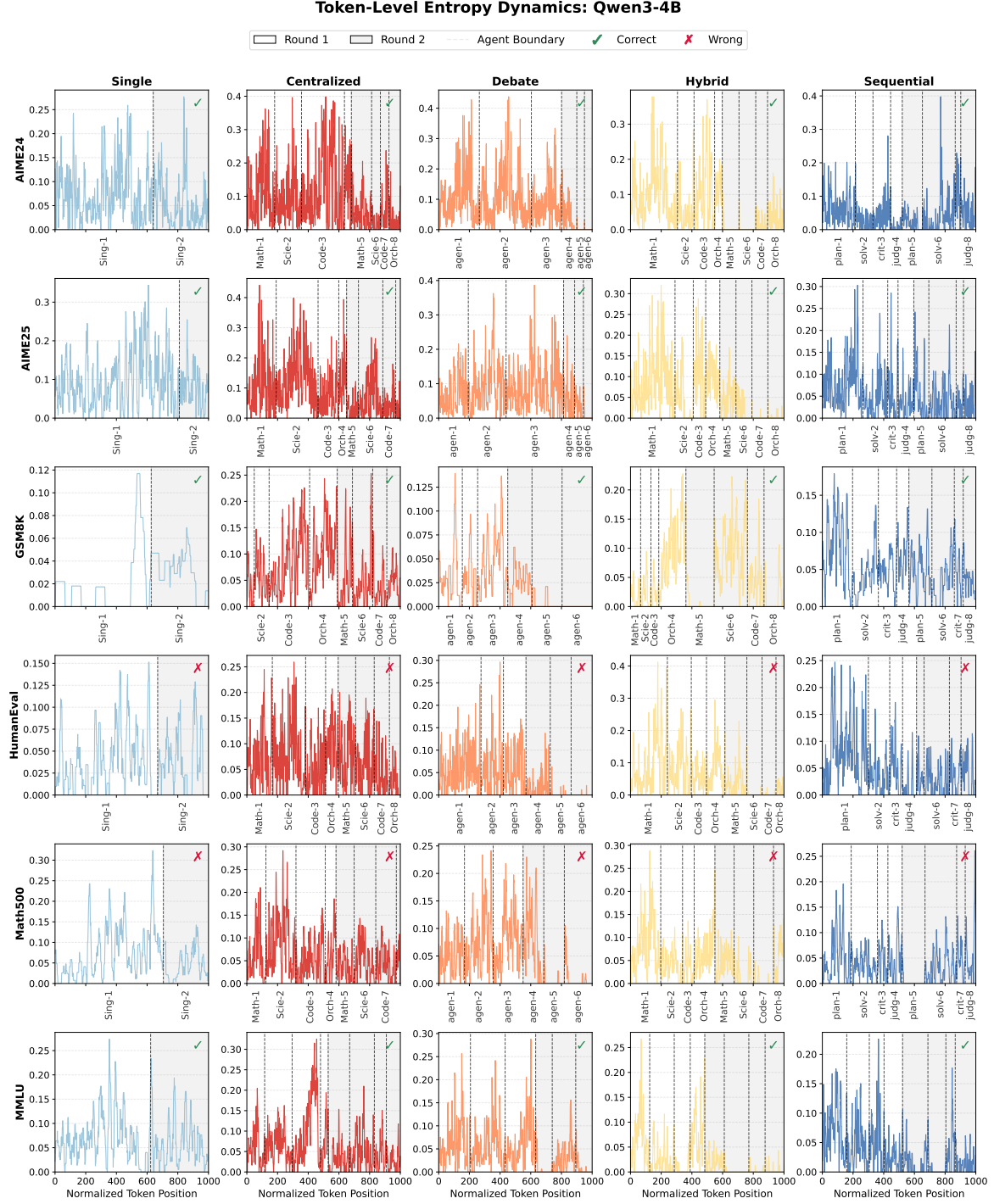


Figure 18. Token-level entropy dynamics for Qwen3-4B. Increased model capacity yields more stable entropy on easier tasks, while harder tasks still induce erratic uncertainty patterns.

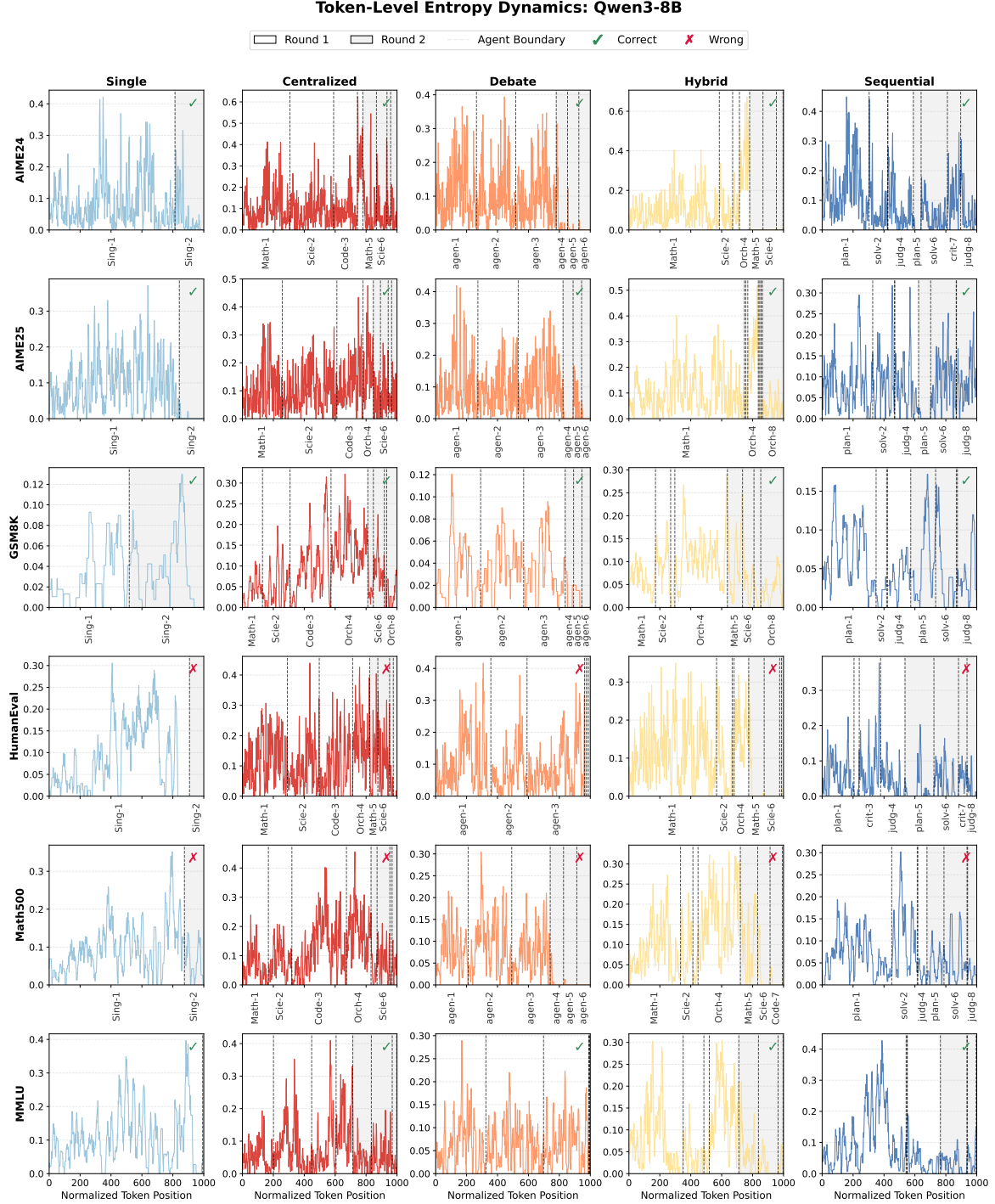


Figure 19. Token-level entropy dynamics for Qwen3-8B. The largest Qwen model shows structured deliberation with controlled exploration in round 1 and smooth convergence in round 2.

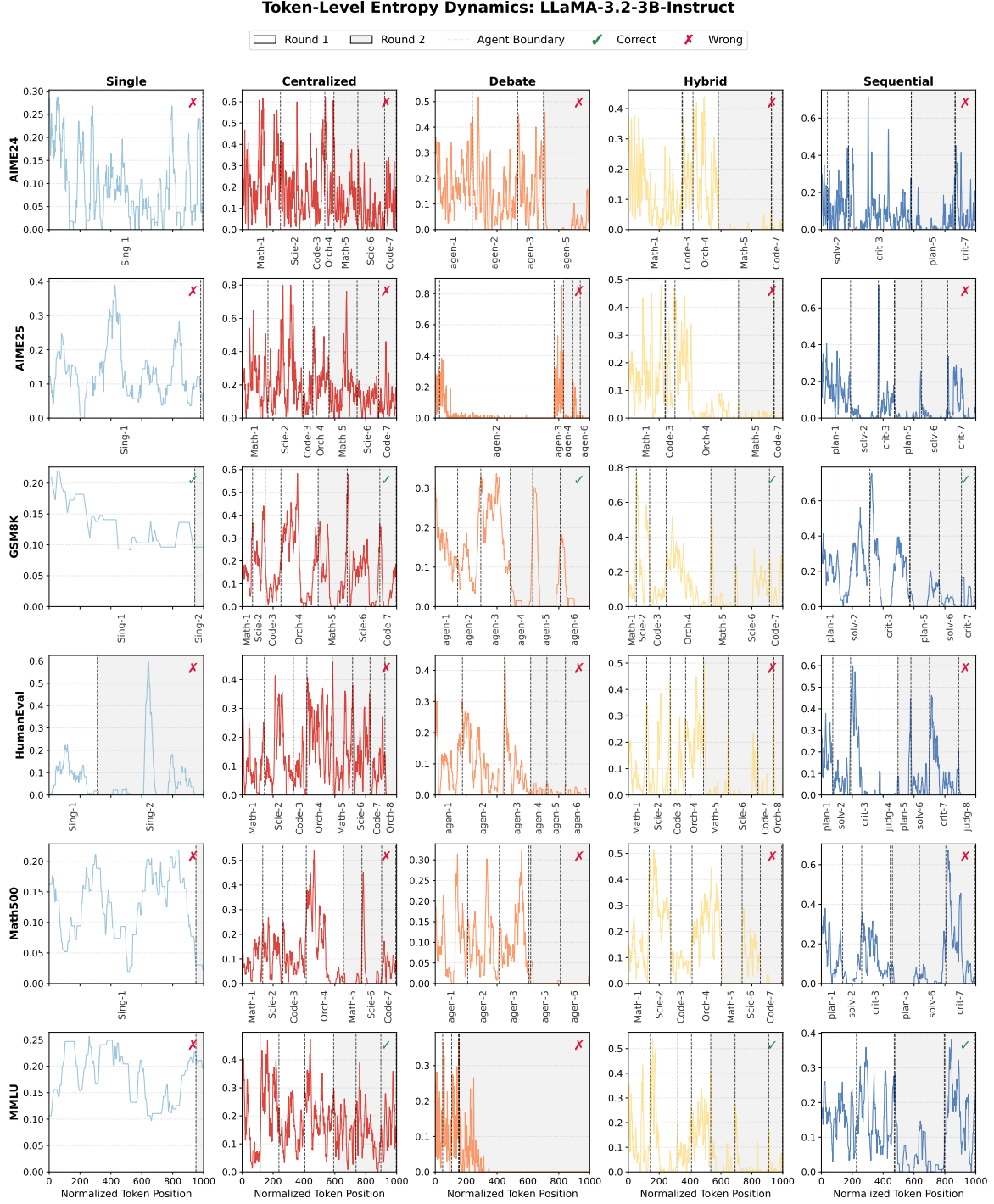


Figure 20. Token-level entropy dynamics for LLaMA-3.2-3B-Instruct. LLaMA exhibits lower round-2 entropy compared to Qwen, often collapsing to near-zero, reflecting a more decisive but potentially overconfident reasoning style.

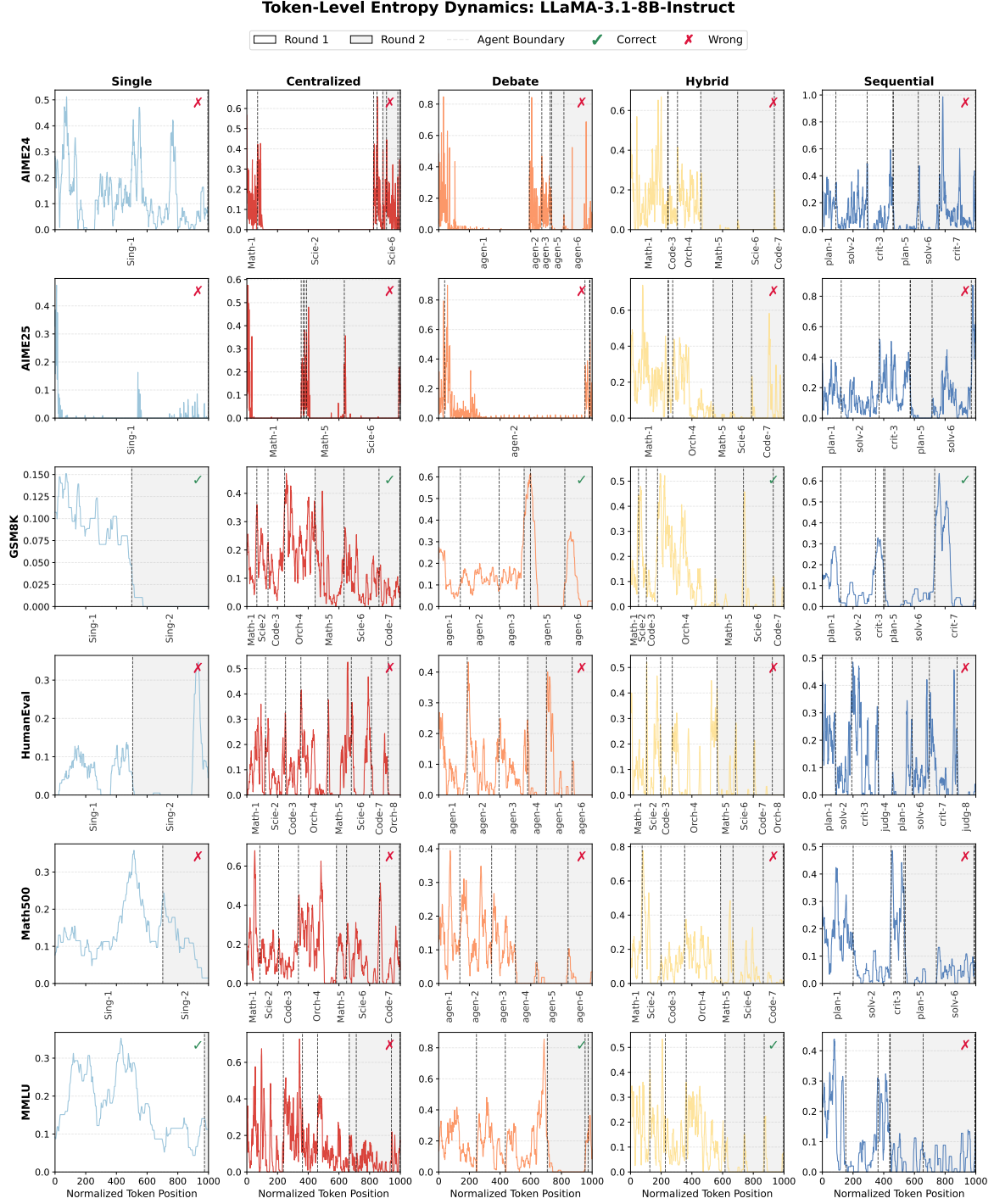


Figure 21. Token-level entropy dynamics for LLaMA-3.1-8B-Instruct. Scaling improves calibration, but the characteristic rapid entropy reduction in round 2 persists compared to Qwen models.